nature portfolio

Peer Review File

Engineered model of heart tissue repair for exploring fibrotic processes and therapeutic interventions

REVIEWER COMMENTS

Reviewer #1 (Remarks to the Author):

In the current manuscript, Yang et al. describe an in vitro model of myocardial infarction using human engineered cardiac tissue (hEHT-MI). Using immunostaining, electrophysiological profiling, and single cell transcriptome, the author demonstrates that hEHT-MI can mimic to some extent the injury response of the heart after MI. The author further demonstrates that the hEHT-MI model could be adapted for high throughput drug screening. By screening reported chemical activators and inhibitors of signaling pathways involved in the post-MI injury response, the author identified a combination of three small molecules, SB431542, Y27632, and CHIR99021, to rescue myocardial dysfunction post-MI in both in vitro and in vivo models. Overall, this manuscript presents a novel in vitro system that can be adapted for high throughput screening to model human myocardial infarction. However, major conceptual and technical concerns arise in spite of the novelty and potential future impacts from this work.

First, the ability of this hEHT-MI platform (at least in its current version) to model human MI is not convincing. To date, there is no established protocol for obtaining adult-like CM from in vitro differentiation. The fact that the CM4 group is still actively proliferating (Figure 3B,3C) further lowers the confidence of using the hEHT-MI model to mimic MI, mainly because in the adult human heart cardiomyocyte rarely goes back to a proliferative state after MI. In fact, this is a challenging task for the whole field. The author may consider extending the differentiation time and adding PGC1a agonist to facilitate maturation of differentiated cardiomyocyte. If extending the culture time is not feasible, some form of selection (such as Cd36 surface marker selection) should be performed to enrich for mature cardiomyocytes.

Another technical concern with the current hEHT MI model is the use of the cone-shaped tips for cryoinjury. For the in vivo cryoinjury model, the tip is usually blunt-ended to avoid structural damage to the cardiac tissue (a better simulation for human MI). Will the penetration itself induce injury response such as fibroblast proliferation? It would be helpful to justify the design if the author could show the difference in terms of cellular response to the puncture with or without freezing the tip.

In Figure 3, the author has performed single cell analysis for both the cryo and control samples. It is interesting to see that no cyro-specific cluster was identified from the analysis. I would suggest that the author integrate the cyro and control datasets using Harmony. Based on Supplementary Figure 6A, it is interesting to see more cells undergoing apoptosis in the control group compared to the cryoinjury group. Based on the gene expression heatmap in Figure S6 and S7, the gene expression profile for Cryo and Con within a cell cluster is very different. Therefore, the author should revisit their data integration method between Con and Cryo to ensure that the cluster is correctly assigned between different treatment groups. More detailed analyses should also be performed. For example, performing gene regulatory network analysis to identify the upstream regulators in the injury response CM/CF clusters. Since the author also performed time-course single cell

experiments between early and late, I would also suggest that they investigate cell fate transition and temporal gene dynamics using pseudotime analysis.

The last concern relates to the design of the in vivo MI experiment (Figure 7). Given the different mechanisms for each small molecule, the author performed the combination treatment by sequentially dosing the mouse with three small molecules. In order to make a meaningful comparison between a single factor and the combination treatment, the author should also only dose the single small molecule in the same time frame as the combination methods. Otherwise the author cannot exclude the possibility that the side effect generated by given small molecules at the wrong time is the reason why the single factor performed much worse than the combination. Also, given the immaturity of the ES/iPS differentiated cells, a more relevant model comparable to the hEHT-MI would be the neonatal mouse cryoinjury model instead of the current adult mouse LAD ligation model.

Reviewer #2 (Remarks to the Author):

In the manuscript by Yang & Zhu et al, the authors created an engineered heart tissue injury model whereby an organoid was created by a patch of hPSC (some from H9, some from hiPSC from gladstone) derived cardiomyocytes and fibroblast mixture. Subsequently, the authors created a cryoinjury model that is meant to mimic myocardial infarction and "regeneration" by watching CM and fibroblast grow back into the region of injury. The authors demonstrated this EHT cryoinjury model can mimic certain aspect of human myocardial scar, including ECM deposition, electrical alteration, and calcium handling. Single cell RNAseq revealed different population of CM and FB. The author subsequently performed a mini screen of 17 compounds, and created a high-content score that identified 3 compounds being "better." Then they treated a small number of murine MI models with these three compounds and in combination, which revealed small improvement in combination but not alone.

Overall, this is a very interesting and creative use of EHT, which could very well have important translational utility, or as a model to study iPSC derived CM proliferation and interaction with FB. However, the proliferative nature of iPSC derived CM compared to actual adult CM makes it much less attractive of a model for clinical MI, which may ultimately limit its utility. Furthermore, other critical players of scar formation, such as inflammatory cells, as well as vascular cells are not included in the EHT, further limiting its potential. The authors though, should be lauded for the creative approach. I would suggest toning down what this model actually represent (it is hardly an MI model), but focus on how it's a great platform to understand FB/CM crosstalk and their regulators. And increase additional details about the biologicl insights one can gain from this model, especially combining scRNAseq and their model with the drug treatment, with in vivo validataion, which could make this a very powerful approach all together.

A few additional specific questions:

1. From the scRNA data, are the fraction of different CM and FB changed with and without injury and over time?
2. Are these different clusters simply reflect cells from different distance to injury site? Or are they truly heterogeneous? validation with some spatial techniques or staining could be informative.
3. Is there any evidence any specific population identified is responsible for response to injury?
4. How does your drug specifically affect these specific clusters?
5. How do the transcriptome of each population of cells in your EHT change with these drug treatments
6. Do the transcriptomic changes in the EHT reflect those seen in the MI model in vivo? I.e. how well does the EHT captures the biology as claimed?
7. Has the authors tried other 3-factor combinations from the original screen? Or are the three factors chosen because they each had some perceived partial benefits, so combination must be better? This three-compound approach is highly unlikely to be translatable.
8. All three compounds seems to significantly reduce infarct size! That's quite impressive (figure 7F). What's the P value for those other ones? Has this been confirmed?
9. How are the 17 candidates chosen? it just says 17 compound in altered pathways from RNAseq. 3/17 hits are quite incredible for any pharmacological screen for phenotype even for one pathway. What does that say about the model's sensitivity and specificity? can you utilize any positive or negative controls?
10. Beyond contractility, are the electrical / calcium phenotype also restored around the scar in the MI model with drug treatment?

Minor:
Line 359 "control of XYZ?" typo?
Line 431: Though the single-factor treatment could improve EF and FS… but your data showed NS… is this a typo?

Reviewer #3 (Remarks to the Author):

In this manuscript, Yang et al. demonstrated a novel human pluripotent stem cell-derived engineered heart tissue patch (hEHT-MI, cryoinjured hEHT model) to mimicking the post-MI pathological remodeling and electrophysiological malfunction, which can be potentially used for screening for anti-fibrotic and cardiac regeneration drugs. RNA sequencing analysis revealed a significant difference in gene expression patterns/signaling pathways at different remodeling periods of cryoinjured hEHT. Single-cell RNA sequencing of CMs and CFs indicates the different signaling pathways, like TGFb, PI3K/AKT, WNT, NFkB, cAMP, RHO and MAPK signaling pathways, play a significant role in fibrotic process, which may be potential therapeutic targets for post-MI cardiac remodeling. Using in vitro mini hEHT-MI model and in vivo mice MI model, they demonstrated the therapeutic benefit of combination treatment with TGFb inhibitor (SB431542),

Rho-kinase inhibitor (Y27632), and WNT activator (CHIR99021), which could restore post-injury myocardial functional.

Overall, the study developed an in vitro humanized cardiac screening platform to develop potential protective drugs against ischemic heart disease. The manuscript is very well written and the experiments are appropriately conducted to justify the findings, which support their conclusion. I have few minor suggestions to improve the manuscript for publication.

1. Please define the abbreviation “PDMS” in the line 133.

2. In the Figure 1D, TUNEL positive cells are hard to be identified in the picture (in gray color), but in Figure 1E, % of TUNEL positive cells are above 20% in remodeling area and 10% in uninjured area. Please improve the quality of the picture for confirming the Figure 1E.

3. In line 164, collagen I is missing in “with increased deposition of collagen and III”.

4. Please explain why both the PI3K activator, 740YP and PI3K inhibitor, LY294002, could significantly accelerate the remodeling processes (Fig. S8C).

5. In figure 7E and F, % infarct size was calculated as % of total left ventricle wall area. They should provide the % of Risk area.

Black text indicates reviewer critique.

Blue text indicates responses or manuscript revisions. All new inclusions in the Revised Manuscript are highlighted in red.

Point-by-point response to Reviewer #1:

Q1-0: In the current manuscript, Yang et al. describe an in vitro model of myocardial infarction using human engineered cardiac tissue (hEHT-MI). Using immunostaining, electrophysiological profiling, and single cell transcriptome, the author demonstrates that hEHT-MI can mimic to some extent the injury response of the heart after MI. The author further demonstrates that the hEHT-MI model could be adapted for high throughput drug screening. By screening reported chemical activators and inhibitors of signaling pathways involved in the post-MI injury response, the author identified a combination of three small molecules, SB431542, Y27632, and CHIR99021, to rescue myocardial dysfunction post-MI in both in vitro and in vivo models. Overall, **this manuscript presents a novel in vitro system that can be adapted for high throughput screening to model human myocardial infarction**. However, major conceptual and technical concerns arise in spite of the novelty and potential future impacts from this work.

R1-0: We sincerely value your expertise and appreciate your insightful comments. Your view of our model as " a novel in vitro system" was a great encouragement to us. In response, we have diligently and comprehensively incorporated new experimental data and in-depth discussions into the revised manuscript to address your concerns. Please refer to the point-by-point response below for a detailed description of our revisions.

Q1-1: First, the ability of this hEHT-MI platform (at least in its current version) to model human MI is not convincing. **To date, there is no established protocol for obtaining adult-like CM from in vitro differentiation.** The fact that the CM4 group is still actively proliferating (Figure 3B,3C) further lowers the confidence of using the hEHT-MI model to mimic MI, mainly because in the adult human heart cardiomyocyte rarely goes back to a proliferative state after MI. **In fact, this is a challenging task for the whole field.** The author may consider extending the differentiation time and adding PGC1a agonist to facilitate maturation of differentiated cardiomyocyte. If extending the culture time is not feasible, some form of selection (such as Cd36 surface marker selection) should be performed to enrich for mature cardiomyocytes.

R1-1: Thank you for your fair review and for pointing out that improving the maturity of hPSC-derived cardiomyocytes (hPSC-CM) to the adult level is the current technical difficulty in the field. The combination of the fibrin hydrogel and dynamic culture in human-engineered heart tissue (hEHT) can significantly enhance its maturation which is comparable to adult heart tissue in contractility and electrical conduction properties[1,2]. We have tried to extend the CM differentiation time and the EHT culture time, but neither approach can fully achieve the properties of injury repair in adult myocardial. Meanwhile, given the large number of mature CM required to fabricate hEHT (1.0 million cells for a hEHT, 3 million cells for a batch of mini hEHTs), the reduction of the number of cells due to the sorting process will be the technical problems that we need to solve in the next phase of the model development.

References:

1. Zhang D, Shadrin IY, Lam J, Xian HQ, Snodgrass HR, Bursac N. Tissue-engineered cardiac patch for advanced functional maturation of human ESC-derived cardiomyocytes. *Biomaterials* **34**, 5813-5820 (2013).

2. Shadrin IY, *et al.* Cardiopatch platform enables maturation and scale-up of human pluripotent stem cell-derived engineered heart tissues. *Nat Commun* **8**, 1825 (2017).

Q1-2: Another technical concern with the current hEHT MI model is the use of the cone-shaped tips for cryoinjury. For the in vivo cryoinjury model, the tip is usually blunt-ended to avoid structural damage to the cardiac tissue (a better simulation for human MI). Will the penetration itself induce injury response such as fibroblast proliferation? It would be helpful to justify the design if the author could **show the difference in terms of cellular response to the puncture with or without freezing the tip.**

R1-2: Thank you for your valuable comments**.** The thickness of the hEHT is approximately 200μm (**fig. S14A, original fig.9A**), thinner than the natural heart wall. Our goal is to create a cryoinjury model with a stable and controllable injured area. We have designed and tested different tips with different shapes to achieve this. We found that blunt tips resulted in uncontrollable cryoinjured areas (**fig S1, E to G**).

Per your suggestion, we compared the difference between inducing injury to hEHT with or without the frozen tip. The frozen tip induced more intense apoptosis around the injury area (**fig. S2, F, and G**). In addition, only the frozen tip induced the accumulation of cellular reactive oxygen species (ROS) around the injury area compared to the non-frozen tip (**fig. S2, H, and I**). This accumulation is considered a critical activator of subsequent fibroblast-mediated myocardial remodeling, suggesting that cryoinjury with the frozen tip activates the hEHT injury repair response. Corresponding results have been added **on Lines 149 to 151 on Page 7 in the revised manuscript**:

"Notably, only the cryoinjury but not puncture can induce dramatic cell apoptosis (**fig. S2, F, and G**) and ROS accumulation (**fig. S2, H and I**) around the injured area."

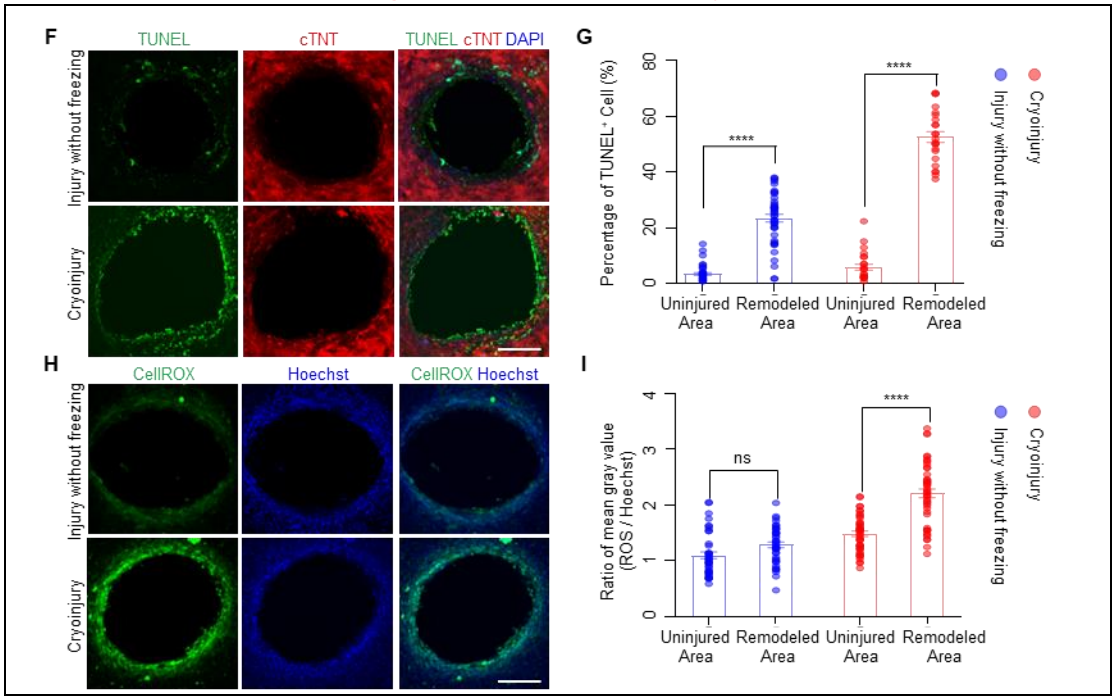

Figure S2. Cryoinjury rather than penetrating injury induced regional cellular apoptosis and ROS accumulation in hEHT. (F) Representative immunofluorescence images of injured hEHT through the unfrozen (top) or frozen tip (bottom) to show the apoptotic cells around the remodeled area. Scale bar, 200μm. (G) Differences in TUNEL+ cells in the uninjured and remodeled area of injured hEHTs. n=30 areas per group. (H) CellROX and Hoechst staining images of injured hEHT through the unfrozen (top) or frozen tip (bottom). Scale bar, 200μm. (I) Differences in ROS accumulation in the uninjured and remodeled area of injured hEHTs. n=40 areas per group.

Q1-3: In Figure 3, the author has performed single cell analysis for both the cryo and control samples. It is interesting to see that no cyro-specific cluster was identified from the analysis. **I would suggest that the author integrate the cyro and control datasets using Harmony.** Based on Supplementary Figure 6A, it is interesting to see more cells undergoing apoptosis in the control group compared to the cryoinjury group. Based on the gene expression heatmap in Figure S6 and S7, the gene expression profile for Cryo and Con within a cell cluster is very different. Therefore, the author should revisit their data integration method between Con and Cryo to ensure that the cluster is correctly assigned between different treatment groups. More detailed analyses should also be performed. For example, **performing gene regulatory network analysis to identify the upstream regulators in the injury response CM/CF clusters.** Since the author also performed time-course single cell experiments between early and late, I would also suggest that they **investigate cell fate transition and temporal gene dynamics using pseudotime analysis.**

R1-3: Thank you for your detailed evaluation and professional advice on our single-cell transcriptomics analysis. As you suggested, we first clustered the cryo and control datasets using Harmony for four iterations and reached convergence, and the tSNE plot showed that the cryoinjury did not create new subpopulations (**fig. S5, D and E**). The following text has been added **on Lines 232 to 234 on Page 12 in the revised manuscript:**

"Further debatching was performed in our scRNA sequencing database using Harmony, and the data reached convergence after 4 iterations of flexibility. Still, no injury-specific clusters were found in four groups (**fig. S5, D and E**)."

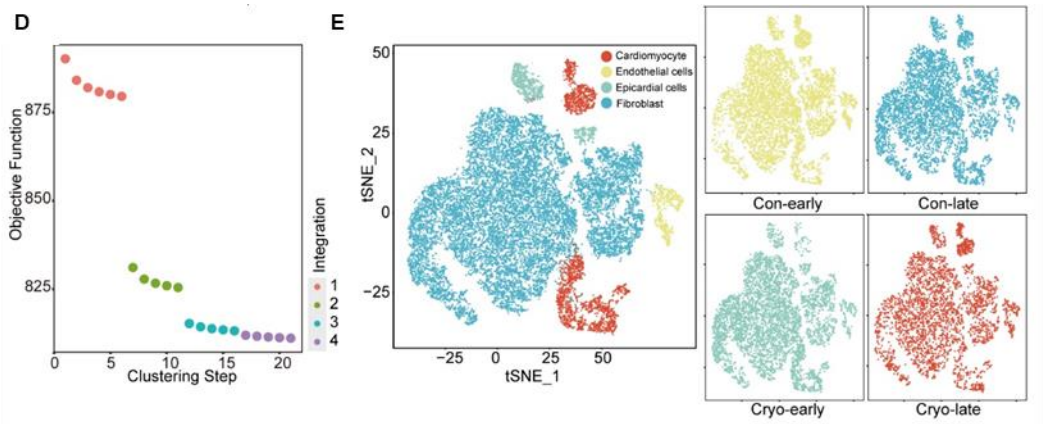

Figure S5. Clustering analysis in the scRNA sequencing dataset of the hEHT injury repair

model. (D) Plot showing the convergence of the Harmony integration process, with stim as the variable to harmonize. Each point represents the cost measured after one round of clustering, with different colors indicating different harmony iterations. The x-axis represents the number of iterations, and the y-axis represents the objective cost. (E) Feature UMAP plots showing the 4 main cell clusters in control and remodeled hEHT at early and late periods. The clustering UMAP plots of different groups were shown on the right side after de-batching by Harmony.

To identify the upstream regulators of CM and CF subpopulations during the remodeling process, we performed transcription factors (TF) analysis and added the relevant results of CM **on Lines 299 to 305 on Page 14 in the revised manuscript:**

"Furthermore, transcription factor (TF) analysis revealed that the upregulated TFs in four CM subpopulations were associated with hypoxic stress (*STAT5A*[50], *BHLHE40*) and anti-apoptosis (*E2F6*, *E2F8*, *NFE2L1*) in the early period (**fig. S8, A and B**). TFs associated with regulation of cardiac development (*ETS1*, *SP2*[51], *MSX2*) and CM proliferation (*E2F7*, *E2F8*) were more pronounced in the late period (**fig. S8, C and D**), suggesting that the stress-activated the potential endogenous regenerative properties of CM in the hEHT injury repair model."

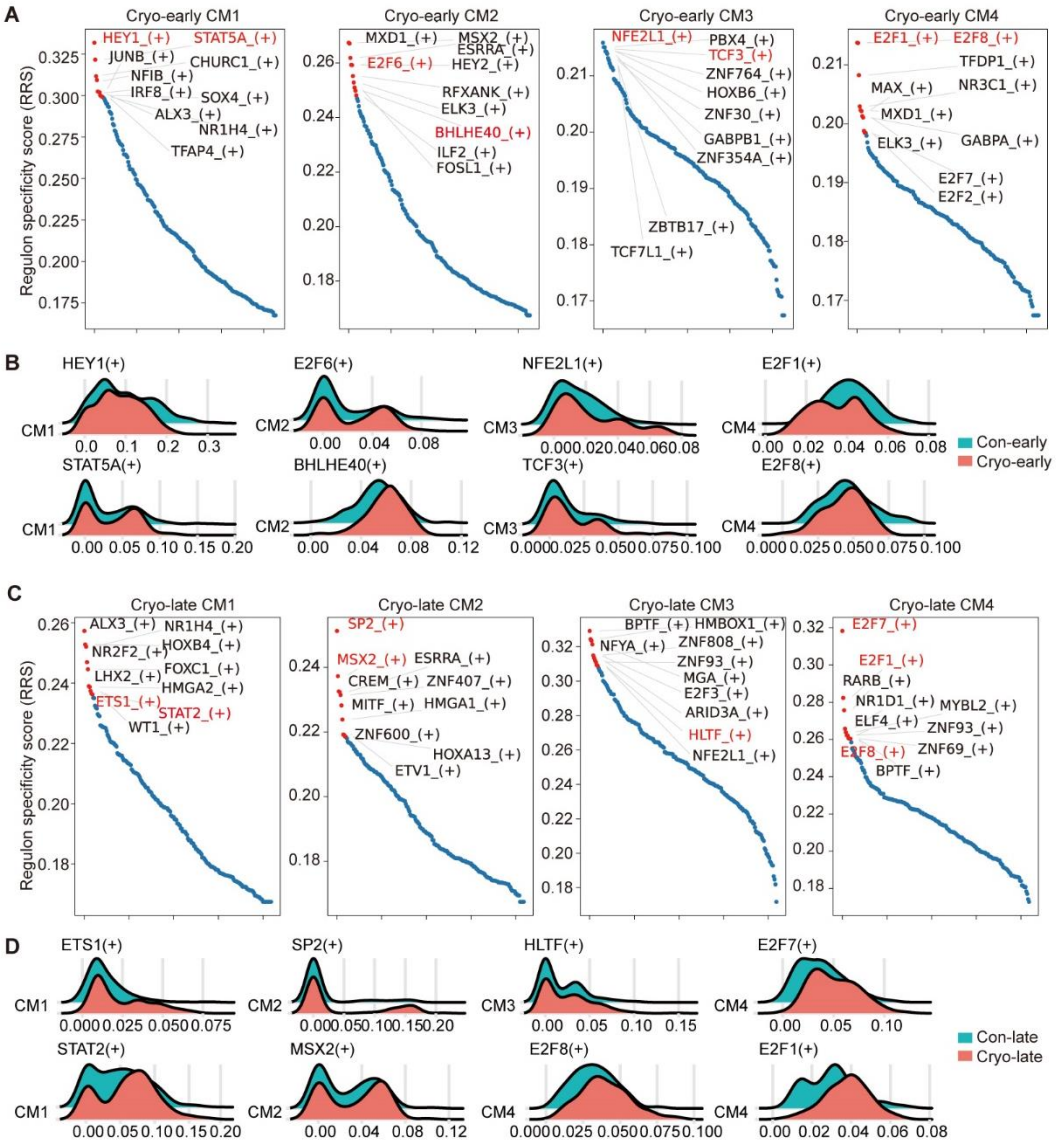

Figure S8. Transcription factor analysis of different CM subpopulations at early and late periods of remolding. (A) Top 10 transcription factors (TF) identified in four CM subpopulations at an early period of remodeling. The x-axis represented individual regulons, while the y-axis showed the Regulon Specificity Score (RSS) values, indicating the specificity of each TF to the corresponding cell subpopulation. (B) Ridgeline plot illustrating the TF activity levels in the specific CM subpopulations in the control and cryoinjury hEHT at early period. Each ridge represented the activity distribution of a TF within a specific cell type. The x-axis indicated the RSS, while the y-axis represented the cell types. (C) Top 10 TF identified in four CM subpopulations at late period of remodeling. (D) Ridgeline plot illustrating the TF activity levels in the specific CM subpopulations in the control and cryoinjury hEHT at late period.

The following articles were newly listed as **references**

"50. Heusch G, Musiolik J, Kottenberg E, Peters J, Jakob H, Thielmann M. STAT5 activation and cardioprotection by remote ischemic preconditioning in humans: short communication. *Circ*

Res **110**, 111-115 (2012).

51. Cui M, *et al.* Transcription factor NFYa controls cardiomyocyte metabolism and proliferation during mouse fetal heart development. *Dev Cell* **58**, 2867-2880 e2867 (2023)."

TF analysis targeting CF in both early and late stages of the hEHT injury repair model was added **on Lines 316 to 322 on Pages 16 to 17 in the revised manuscript:**

"TF analysis for the CF subpopulation showed that the levels of proliferation-associated TFs *E2F7*[56], *E2F8*, and *E2F1*[57] were decreased in proliferative CF1 in the early period (**fig. S10, A and B**) but then increased in the late period (**fig. S10, C and D**). Similarly, CF4 and CF5 highly expressed TF associated with cell fate transition in the early period, such as *PBX4*[58] and *FOSL2*[59] (**fig. S10, A and B**), but had lower expression of *MSX1* in the late period (**fig. S10, C and D**), indicating that this injury-induced fate transition in inactive CF was progressively attenuated and eventually contribute to the fibrotic scar."

The following articles were newly listed as **references**

"56. Westendorp B, Mokry M, Groot Koerkamp MJ, Holstege FC, Cuppen E, de Bruin A. E2F7 represses a network of oscillating cell cycle genes to control S-phase progression. *Nucleic Acids Res* **40**, 3511-3523 (2012).

57. Liao R, Xie B, Cui J, Qi Z, Xue S, Wang Y. E2F transcription factor 1 (E2F1) promotes the transforming growth factor TGF-beta1 induced human cardiac fibroblasts differentiation through promoting the transcription of CCNE2 gene. *Bioengineered* **12**, 6869-6877 (2021).

58. Holowiecki A, Linstrum K, Ravisankar P, Chetal K, Salomonis N, Waxman JS. Pbx4 limits heart size and fosters arch artery formation by partitioning second heart field progenitors and restricting proliferation. *Development* **147**, (2020).

59. Stellato M, *et al.* The AP-1 transcription factor Fosl-2 drives cardiac fibrosis and arrhythmias under immunofibrotic conditions. *Commun Biol* **6**, 161 (2023)."

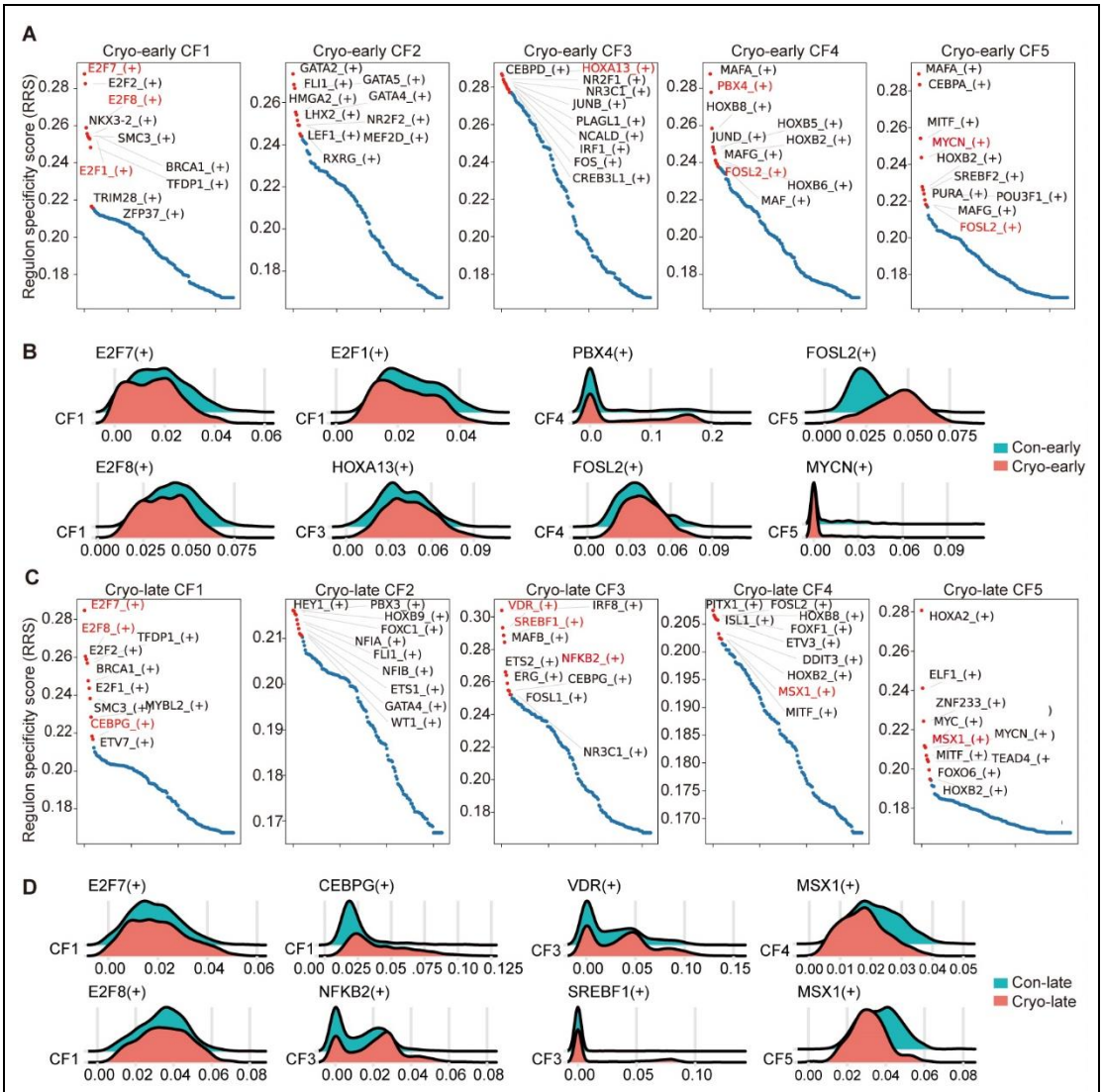

Figure S10. Transcription factor analysis of different CF subpopulations at early and late periods of remolding. (A) Top 10 transcription factors (TF) identified in five CF subpopulations at the early period of remodeling. The x-axis represented individual regulons, while the y-axis showed the Regulon Specificity Score (RSS) values, indicating the specificity of each TF to the corresponding cell subpopulation. (B) Ridgeline plot illustrating the TF activity levels in the specific CF subpopulations in the control and cryoinjury hEHT at early period. Each ridge represented the activity distribution of a TF within a specific cell type. The x-axis indicated the RSS, while the y-axis represented the cell types. (C) Top 10 TF identified in five CF subpopulations at late period of remodeling. (D) Ridgeline plot illustrating the TF activity levels in the specific CF subpopulations in the control and cryoinjury hEHT at late period.

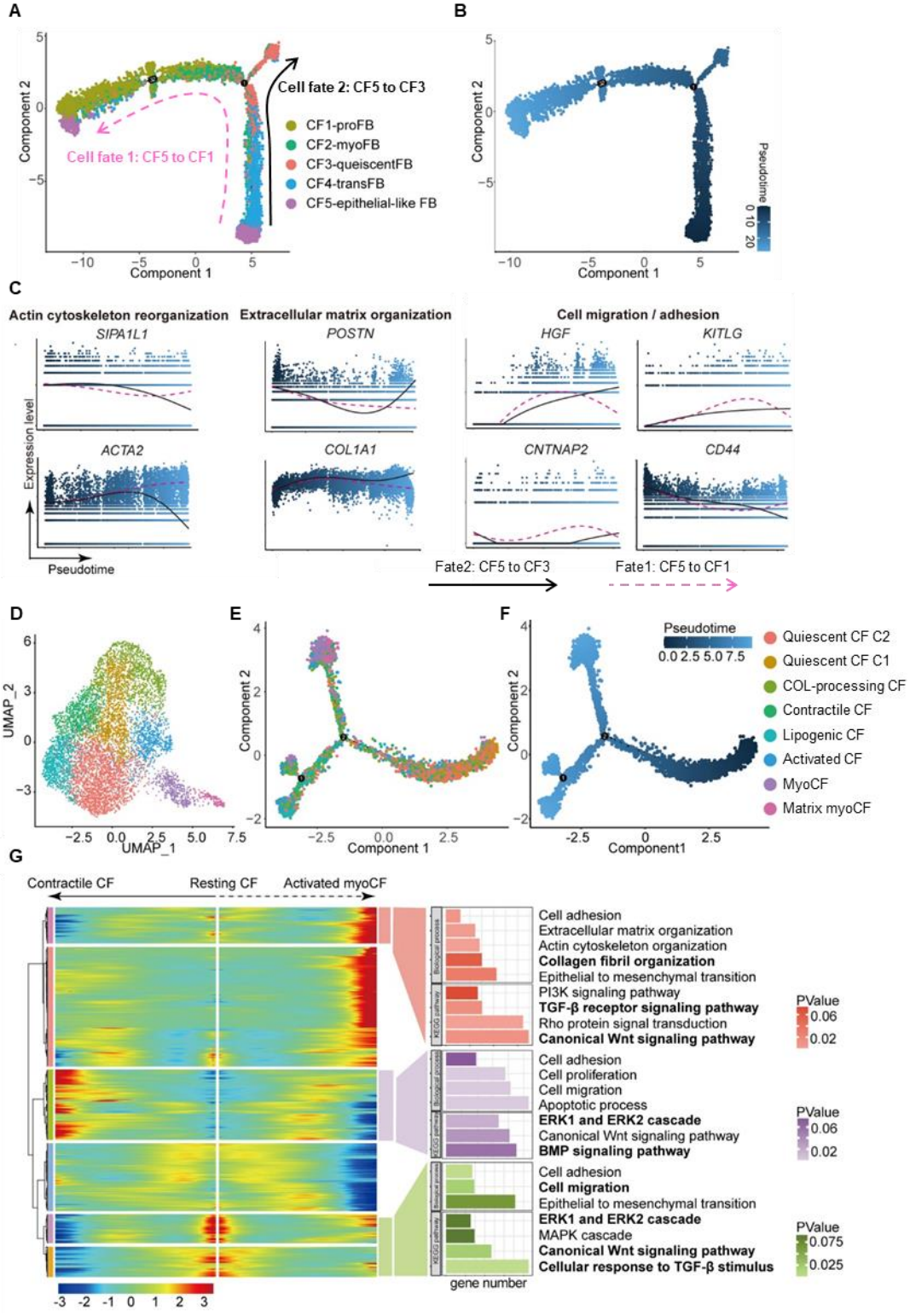

Figure S11. Pseudotime analysis of CF subpopulations in the hEHT injury repair model and clinical DCM/ICM hearts. (A) Distinct states of CF subpopulations identified by pseudotime analysis in the hEHT injury repair model. (B) Pseudotemporal trajectory plot of CF in the hEHT injury repair model. (C) Spline plots of representative genes changed in two CF transition trajectories in the hEHT injury repair model. The black line indicated the gene

expression change from CF5 to CF3 and the pink dashed line indicated the gene expression change from CF5 to CF1. (D) UMAP plot showing the CF clusters from the scRNA sequencing database of normal, DCM, and ICM hearts (GEO: GSE145154). (E) Distinct states of CF subpopulations identified by pseudotime analysis in clinically normal, DCM, and ICM hearts. (F) Pseudotemporal trajectory plot of CF in clinically normal, DCM, and ICM hearts. (G) Heatmap of significantly changed genes at the transition node (position 2 in (F)) from quiescent CF to activated myoCF or contractile CF. The color from blue to red indicated the relative expression level from low to high. Representative GO terms of the significantly changed gene set in pseudotime trajectory were shown on the right.

We also investigated cell fate transition and temporal gene dynamics using pseudotime analysis **on Lines 328 to 348 on Page 17 in the revised manuscript:**

"CF is dominant in pathological myocardial remodeling, prompting our focus on its fate transitions during injury repair. Pseudotime analysis revealed two lineage trajectories: cell fate 1 from CF5 to CF1 and cell fate 2 from CF5 to CF3 (**fig. S11, A and B**). Three gene sets were identified to modulate the cell fate transitions (**Fig. 4A**), including gene set 1, which was enriched in terms related to cell fate determination, oxidative stress, and WNT, Rho signaling pathways to promote cell fate 2 from CF5 to CF3. Gene set 3 dominated the cell fate transition from CF5 to CF1 and was enriched in BMP, TGFβ, and MAPK signaling pathways (**Fig. 4B**). Specifically, in gene set 3, the cytoskeleton-related genes *SIPA1L1* and *ACTA2* increased in cell fate 1 but decreased in cell fate 2, while the ECM-related genes *POSTN* and *COL1A1* exhibited opposite patterns (**fig. S11C**), indicating the differential modulation in CF fate.

To assess the in vivo relevance of CF fate transition in the hEHT injury repair model, we further referenced the scRNA-seq data from clinical heart with dilated cardiomyopathy (DCM) and ischemic cardiomyopathy (ICM) hearts[34] (**fig. S11D**). Clustering and pseudotime analysis revealed that the quiescent CF in human MI hearts similarly underwent two distinct fates to transition to myoCF or contractile CF (**fig. S11, E and F**), which were regulated by TGFβ, WNT, PI3K, and ERK signaling pathways (**fig. S11G**). The CF in hEHT injury repair model showed similar fate transition patterns, including the dynamic expression of genes associated with TGF-β signaling (*JUN*, *FOS*, *COL3A1*), extracellular matrix (*ADAMTS1*, *COL16A1*, *MMP28*), and stress response (*COL1A1*, *BTG*, *FOSB*) as in vivo (**Fig. 4, C and D**). These results suggested that the hEHT injury repair model effectively captures the biological processes of CF fate transition identified in human MI."

The following article was newly listed as **references**

"34. Rao M*, et al.* Resolving the intertwining of inflammation and fibrosis in human heart failure at single-cell level. *Basic Res Cardiol* **116**, 55 (2021)."

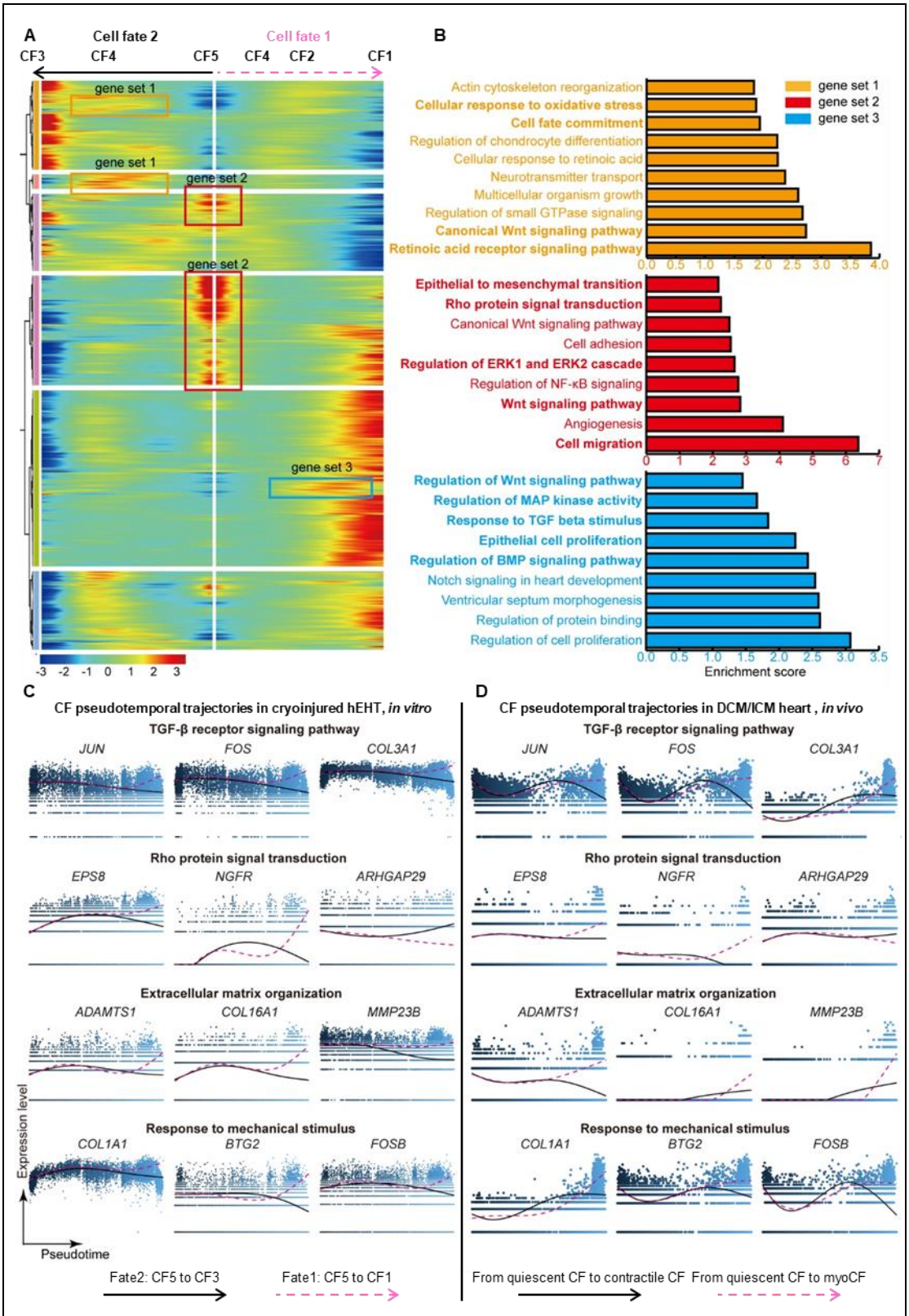

Figure 4. Pseudotime analysis revealed that CF in the hEHT injury repair model exhibited comparable cell fate transitions in vivo. (A) Heatmap of significantly changed genes at the transition node from epicardial-like fibroblasts (CF5) to quiescent fibroblasts (CF3) or proliferative fibroblasts (CF1). The black line indicated the gene expression change from CF5 to

CF3 and the pink dashed line indicated the change from CF5 to CF1. The color blue to red indicates the relative expression level, which ranges from low to high. (B) Top 10 GO terms of significantly changed gene set (different colored frames in (A)) in pseudotime trajectory. (C) Spline plots of representative genes changed in two CF transition trajectories in the hEHT injury repair model. (D) Spline plots of the same genes in (C) that were changed in two CF transition trajectories in the clinically DCM/ICM hearts (GEO: GSE145154). The black line indicated the gene expression change from quiescent CF to contractile CF, and the pink dashed line indicated the change from quiescent CF to myoCF.

These findings revealed the dynamic transition in different cell subpopulations during the hEHT remodeling, providing the field with another angle to understand cardiac tissue repair.

Q1-4: The last concern relates to the design of the in vivo MI experiment (Figure 7). Given the different mechanisms for each small molecule, the author performed the combination treatment by sequentially dosing the mouse with three small molecules. In order to make a meaningful comparison between a single factor and the combination treatment, the author should also **only dose the single small molecule in the same time frame as the combination methods.** Otherwise the author cannot exclude the possibility that the side effect generated by given small molecules at the wrong time is the reason why the single factor performed much worse than the combination. Also, given the immaturity of the ES/iPS differentiated cells, a more relevant model comparable to the hEHT-MI would be **the neonatal mouse cryoinjury model instead of the current adult mouse LAD ligation model.**

R1-4: We understand and share your concern about the potential side effects of administering small molecules in unpaired time points. We update additional in vivo MI experiments with single-factor molecule treatment with paired periods as the combination group (Y27632 on days 1-7, CHIR99021 on days 8-14, and SB431542 on days 15-21.) After 21 days, both Masson staining analysis and echocardiographic assessment show an enhanced structure and function in the combination treatment. The relevant results were added **on Lines 531 to 547 on Pages 30 to 31 in the revised manuscript:**

"Subsequently, we developed the MI model in adult mice and evaluated the therapeutic effects of Y27632, CHIR99021, SB431542, and their combination (**Fig. 8A**). Echocardiography assessment (**Fig. 8B**) revealed that both the ejection fraction (EF) and fractional shortening (FS) significantly decreased in all treated groups compared with the sham-operated group at day 1 post-MI. However, only the combined treatment enhanced cardiac function considerably after 21 days post-treatment compared to the vehicle group (**Fig. 8, C, and D**). The Masson staining analysis (**Fig. 8E**) further showed the combined treatment can significantly reduce the fibrotic area compared to the vehicle group (**Fig. 8F**). Notably, the phased single-factor treatment with CHIR99021 in days 7 to 14 (cardiac replacement fibrosis phase) post-MI also significantly reduced the formation of fibrotic scar (**Fig. 8F**) but failed to rescue the cardiac function (**Fig. 8, C and D**). In contrast, sustained CHIR99021 treatment throughout the remodeling process (21 days post-MI) in adult MI mice (**fig. S19A**) failed to reduce the fibrotic area. In contrast, phased interventions in combination with Y27632, CHIR99021, and SB431542 can still promote functional repair post-MI (**fig. S19, B**

to F), indicating the importance of symptomatic treatment of remodeling stages with different pathological features. The above results further validate that the potential value of the Y27632, CHIR99021, and SB431542 identified from the hEHT injury repair model, their combination can distinctively have a positive impact on MI." fig. S19 is the original Fig. 7.

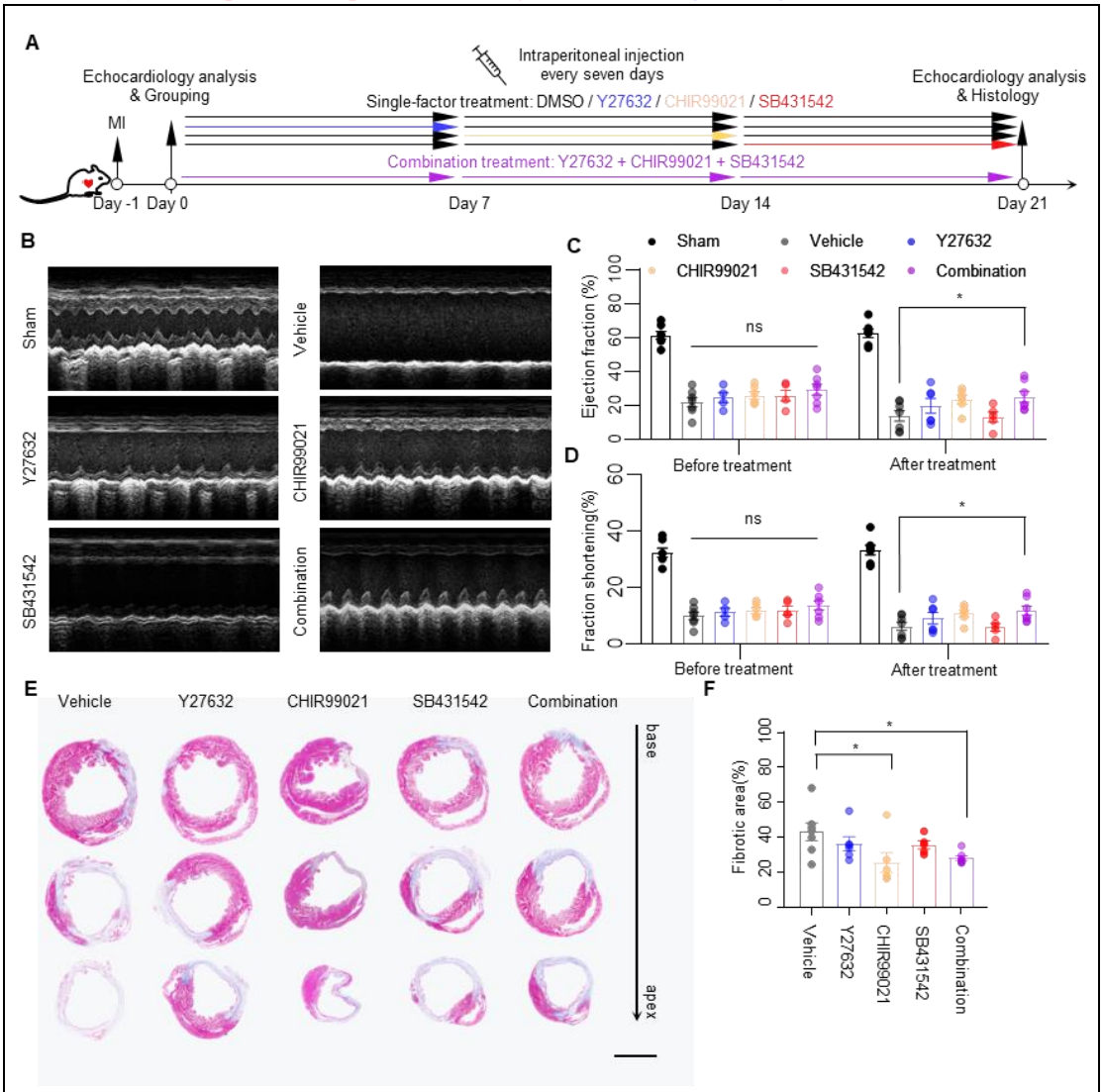

Figure 8. The combination treatment reduced the fibrotic area and improved cardiac function in the adult mouse model of MI. (D) Schematic of different treatments (DMSO, Y27632, CHIR99021, SB431542, and their combination) in adult mice after MI. (E) Representative images of M-code echocardiography from Sham, Vehicle, Y27632, CHIR99021, SB431542, and their combination-treated mice after 21 days of treatment. (F) Ejection fraction measured by echocardiography in different groups of mice before treatment and 21 days after treatment. (G) Fraction shortening measured by echocardiography in different groups of mice before treatment and 21 days after treatment. n=7 mice for Sham, Vehicle and Combination; n=6 mice for Y27632 and CHIR99021; n=5 mice for SB431542. (H) Representative Masson staining images of heart sections from different groups of adult mice at 21 days after treatment. Scale bar,2.5mm. (I) Quantitative analysis of fibrotic area measured from Masson staining image from

different group mice at 21 days after treatment. n = 7 mice for Vehicle and Combination; n=6 for Y27632 and CHIR99021; n = 5 mice for SB431542. ns, not significant; *P < 0.05. **P < 0.01.

Inspired by your suggestion, we established the cryoinjury model in the neonatal mouse. Subsequently, the Y27632, CHIR99021, and SB431542 were separately injected subcutaneously into neonatal mice on days 1-4, 5-8, and 9-12 after the cryoinjury, defined as the combination treatment. Similarly, the single-factor treatment was defined as the injection of small molecules at the same time as the combination treatment. According to the Masson staining results, only the combination treatment can reduce the fibrotic area of the cryoinjured hearts. The relevant results were added **on Lines 515 to 530 on Page 30 in the revised manuscript:**

"Undeniably, immature and proliferating CM subpopulations in our hEHT injury repair model can be essential for initiating regenerative repair after injury, as demonstrated in the cryoinjury model of neonatal mice[18]. The heart of neonatal mice with 15% direct apical excision can fully recover within 21 days, demonstrating its powerful regenerative capacity, but this capacity declines sharply with age[80]. Considering that our model of myocardial injury repair focused more on fibrotic remodeling and screening for related therapeutic targets, we, therefore, performed transmural cryoinjury (penetrating the entire ventricular wall) in neonatal mice at 3 days postnatal age (P3) to induce cardiac healing with fibrotic scarring. Post-MI, the myocardial pathological remodeling process is multi-factor led and highly dynamic in vivo, which includes the early inflammatory phase, cardiac replacement fibrosis phase, and scar maturation phase[3]. Similarly, we validated the effects of Y27632, CHIR99021, and SB431542, these single-factor treatments, and their phased combination treatments on myocardial injury repair in the above cryoinjury model of neonatal mice (**fig. S18A**). After 12 days of treatment, the heart in the vehicle groups showed thinning of the ventricular wall and fibrotic scar filling (**fig. S18B**), while only the combination treatment can preserve the ventricular and significantly reduce the fibrotic area based on Masson staining analysis (**fig. S18C**)."

The following article was newly listed as **references**

"80. Lam NT, Sadek HA. Neonatal Heart Regeneration: Comprehensive Literature Review. *Circulation* **138**, 412-423 (2018)."

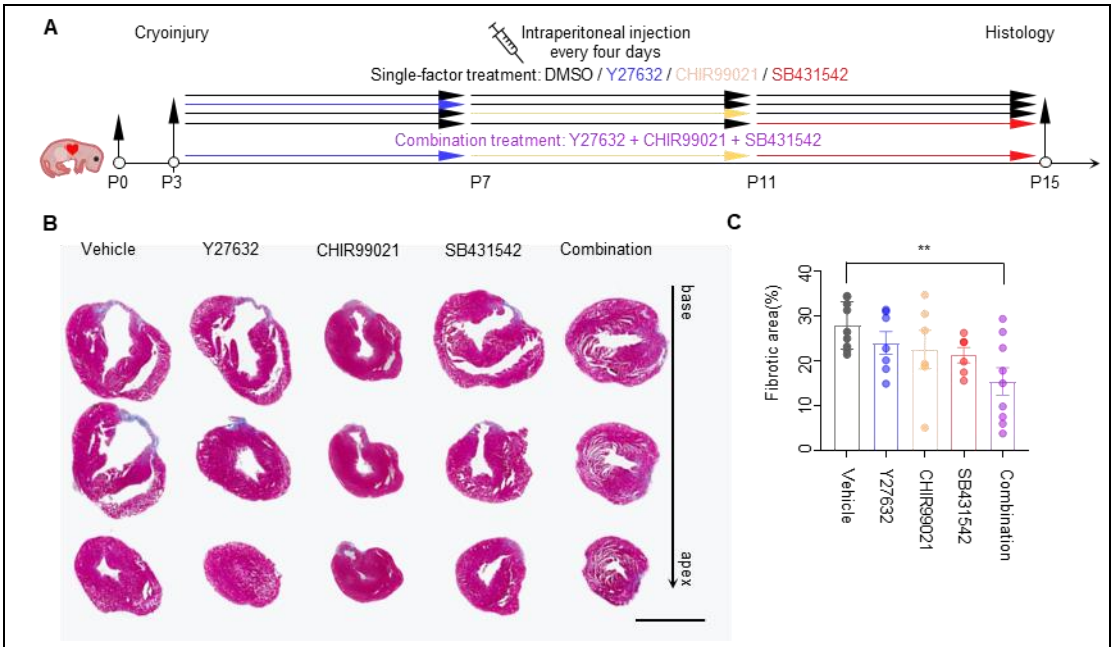

Figure S18. The combination treatment reduced the fibrotic area in the cryoinjured heart of neonatal mice. (A) Schematic of experimental protocol in the cryoinjury model of neonatal mice. The ventricle of neonatal mice was cryoinjured at 3 days of postnatal (P3) and was progressively treated with DMSO (Vehicle) or Y27632, CHIR99021, SB431542, or their combination. (B) Representative Masson staining images of heart sections from cryoinjured neonatal mice at 12 days after single-factor (DMSO, Y27632, CHIR99021, SB431542) or combination treatments. Scale bar, 2.5mm. (C) Quantitative analysis of fibrotic area measured from Masson staining image of mice in different groups at 12 days after treatment. n = 9 mice for vehicle; n=7 mice for Y27632; n=6 for CHIR99021 and SB431542; n = 9 mice for combination.

Point-by-point response to Reviewer #2:

Q2-0: In the manuscript by Yang & Zhu et al, the authors created an engineered heart tissue injury model whereby an organoid was created by a patch of hPSC (some from H9, some from hiPSC from gladstone) derived cardiomyocytes and fibroblast mixture. Subsequently, the authors created a cryoinjury model that is meant to mimic myocardial infarction and "regeneration" by watching CM and fibroblast grow back into the region of injury. The authors demonstrated this EHT cryoinjury model can mimic certain aspect of human myocardial scar, including ECM deposition, electrical alteration, and calcium handling. Single cell RNAseq revealed different population of CM and FB. The author subsequently performed a mini screen of 17 compounds, and created a high-content score that identified 3 compounds being "better." Then they treated a small number of murine MI models with these three compounds and in combination, which revealed small improvement in combination but not alone.

Overall, this is a very interesting and creative use of EHT, which could very well have important translational utility, or as a model to study iPSC derived CM proliferation and interaction with FB. However, the proliferative nature of iPSC derived CM compared to actual adult CM makes it much less attractive of a model for clinical MI, which may ultimately limit its utility. Furthermore, other critical players of scar formation, such as inflammatory cells, as well as vascular cells are not included in the EHT, further limiting its potential. The authors though, should be lauded for the creative approach. I would suggest **toning down what this model actually represent (it is hardly an MI model),** but focus on how **it's a great platform to understand FB/CM crosstalk and their regulators.** And increase additional details about the biologicl insights one can gain from this model, especially combining scRNAseq and their model with the drug treatment, with in vivo validataion, which could make this a very powerful approach all together.

R2-0: Thank you for your accurate and comprehensive description of our work! We are encouraged by your comments that our work is interesting and creative. We sincerely appreciate and accept your point that our model should be a myocardial injury-repair model instead of an MI model. Therefore, we have renamed our model as "hEHT injury repair model" and replaced the previous name with it in the revised manuscript. Meanwhile, we followed your suggestion and investigated the interaction between cardiac fibroblasts (CF) and cardiomyocytes (CM) during the injury repair process based on our scRNAseq database. The relevant results were added **on Lines 349 to 364 on Page 18 in the revised manuscript:**

"Given CF's highly plastic and dynamic nature, we further considered their interactions with other cell subpopulations in our model (**fig. S12A**). Cryoinjury significantly increased the number of CF-CM interactions, particularly between CF2/CF5 and CM, except mature CM3 (**fig. S12B**). In particular, CF2 and CF5 can regulate CM metabolism through APOA1_ABCA1[61] interactions in the early period. CF2 individually secreted TGFB1 to induce CM stress, while CF5 can modulate CM proliferation through NRXN2_DAG1[62] while protecting the heart by regulating glucose uptake and the AMPK pathway via APP_CD74[63] (**fig. S12C**). This potential cardioprotective effect was reversed in the late period, i.e., CF5 may harassed calcium and iron homeostasis to induce CM apoptosis via SEMA4D_PLXNB1[64] and HFE_TFRC[65] interactions (**fig. S12C**). The above scRNA-seq analysis demonstrated the complex dynamic orchestration during the remodeling process of

cryoinjured hEHT, especially in CF with high clinical relevance, which progressively contributed to the final fibrotic scar and dysfunction. These cellular dynamics were mainly dominated by serious signaling pathways such as TGFβ, WNT, RHO, PI3K, NFκB, and MAPK, which allowed us to gain a deeper understanding of the underlying mechanisms in the fibrosis, and these signaling pathways may be promising therapeutic targets in regulating the pathological remodeling of myocardial post-MI."

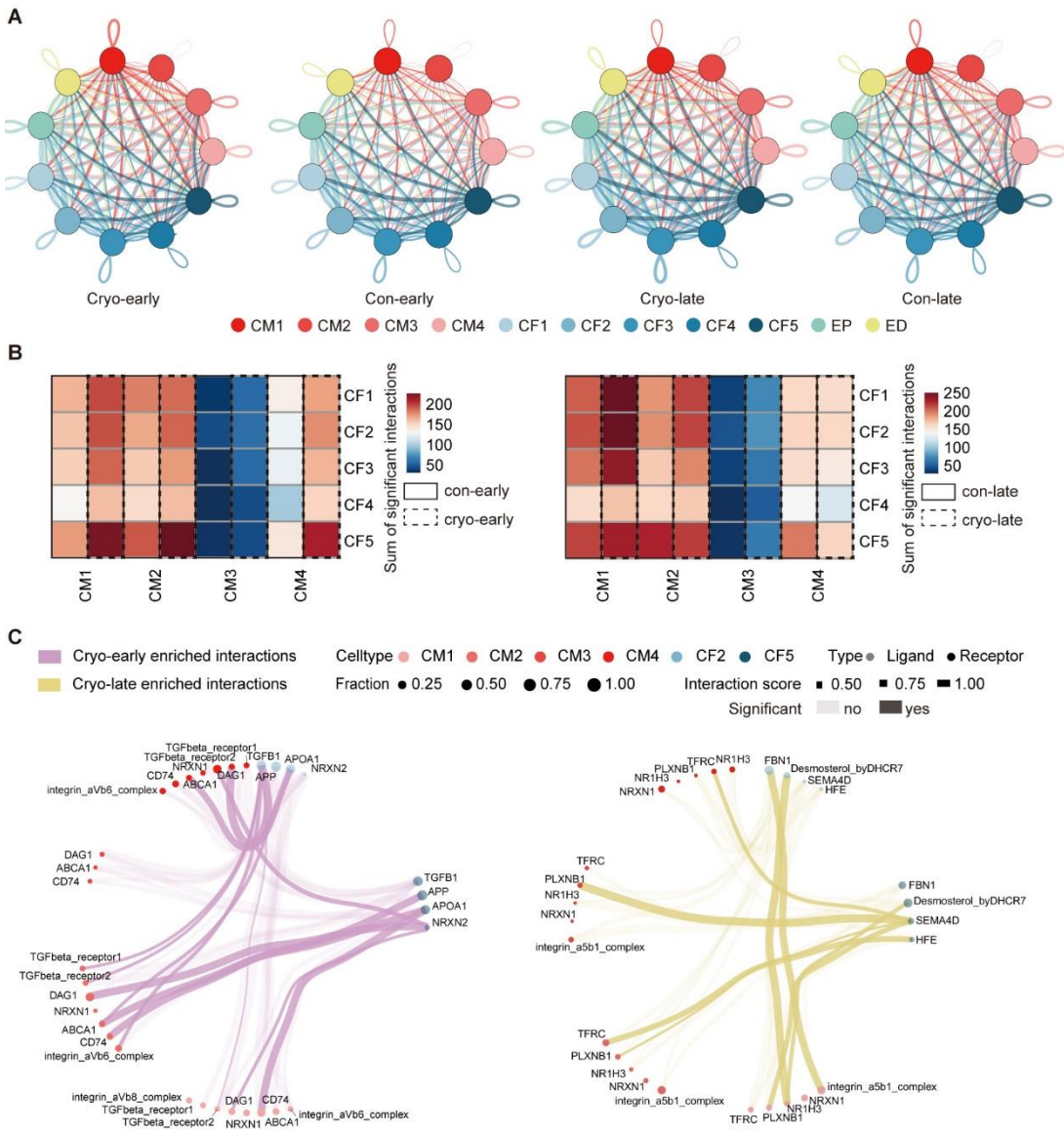

Figure S12. Cellular interactions in the hEHT injury repair model. (A) The interaction network of different cellular subpopulations in control and cryoinjury hEHT at early and late periods. The thickness of the connection lines represented the number of interactions. (B) Heatmap of the number of CF1-5 and CM1-4 interactions in the control and the cryoinjury hEHT. (C) Circle plots of specific cellular interactions in the cryoinjured hEHT at early and late periods.

The following articles were newly listed as **references**

"61. Zhao GJ, Yin K, Fu YC, Tang CK. The interaction of ApoA-I and ABCA1 triggers signal transduction pathways to mediate efflux of cellular lipids. *Mol Med* **18**, 149-158 (2012).

62. Morikawa Y, Heallen T, Leach J, Xiao Y, Martin JF. Dystrophin-glycoprotein complex sequesters Yap to inhibit cardiomyocyte proliferation. *Nature* **547**, 227-231 (2017).

63. Li QL, Tang J, Zhao L, Ruze A, Shan XF, Gao XM. The role of CD74 in cardiovascular disease. *Front Cardiovasc Med* **9**, 1049143 (2022).

64. Sun M, Chen Z, Song Y, Zhang B, Yang J, Tan H. PLXND1-mediated calcium dyshomeostasis impairs endocardial endothelial autophagy in atrial fibrillation. *Front Physiol* **13**, 960480 (2022).

65. Pan Y, Yang J, Dai J, Xu X, Zhou X, Mao W. TFRC in cardiomyocytes promotes macrophage infiltration and activation during the process of heart failure through regulating Ccl2 expression mediated by hypoxia inducible factor-1alpha. *Immun Inflamm Dis* **11**, e835 (2023)."

Q2-1: A few additional specific questions: 1. From the scRNA data, are the fraction of different CM and FB changed with and without injury and over time?

R2-1: According to your valuable suggestion, we analyzed the changes in the percentage of each cell subpopulation in different groups based on scRNA-seq and added this section **on Lines 281 to 288 on Page 14 in the revised manuscript:**:

"In addition to changes in the spatial distribution of different cell subpopulations, cryoinjury also reduced the number of cells captured by scRNA sequencing in hEHT (**fig. S6E**). Specifically, the cryoinjury increased the percentage of immature CM (CM1, CM2) and inactive CF (CF4, CF5), while all other cell subpopulations decreased in the early period (**fig. S6E**). This trend was completely reversed in the late period, with an increase in activated CF1, CF2 and also in proliferating CM3 (**fig. S6E**), which was consistent with the presence of different proportions of CF and CM in the remodeling region (**Fig. 1, G and H**)."

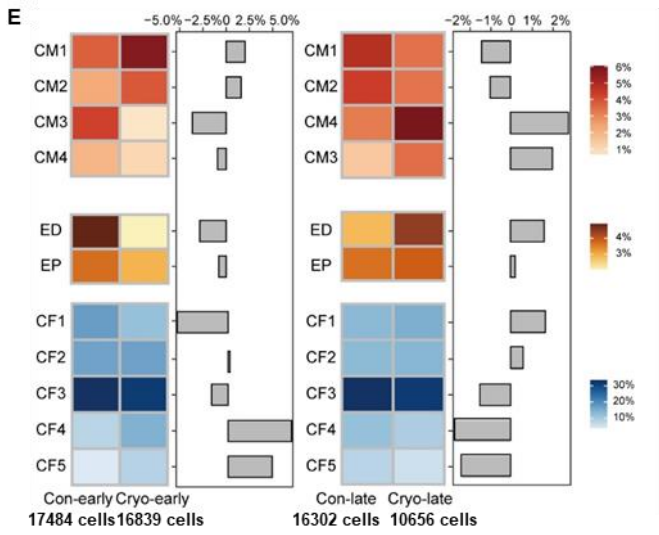

Figure S6. Analysis and characterization of cellular composition in hEHT injury repair model. (E) Heatmap of the percentage of each cell subpopulation in the control and cryoinjury groups at both the early and late period, with the color representing the percentage of different cell subpopulations. Bar graphs showed the change in cell percentage in the cryoinjury group compared to the control group.

Q2-2: 2. Are these different clusters simply reflect cells from different distance to injury site? Or are they truly heterogeneous? validation with some spatial techniques or staining could be informative.

R2-2: There was some spatial heterogeneity of these different clusters, as shown by our immunofluorescence staining results (**Fig.3, H and I**). The $VIM^+/CXADR^+$ CF5 (epicardial-like CF) were mainly distributed in the outer part of the remodeling area, whereas the $VIM^+/CXADR^-$ CF can be further distinguished into $CD44^+$ CF4 (transitional CF) and $CD44^-$ CF1-3 in the remodeling area (**Fig.3, H and I**), indicating that the more quiescent CF were progressively transited to the activated CF and thus contributed to the myocardial remodeling of cryoinjured hEHT.

Q2-3: 3. Is there any evidence any specific population identified is responsible for response to injury?

R2-3: We additionally used Harmony integration for cell clustering. However, we were unable to identify the additional cryoinjury-specific cell subpopulations. The following text has been added **on Lines 232 to 234 on Page 12 in the revised manuscript:**

"Further debatching was performed in our scRNA sequencing database using Harmony, and the data reached convergence after 4 iterations of flexibility. Still, no injury-specific clusters were found in four groups (**fig. S5, D and E**)."

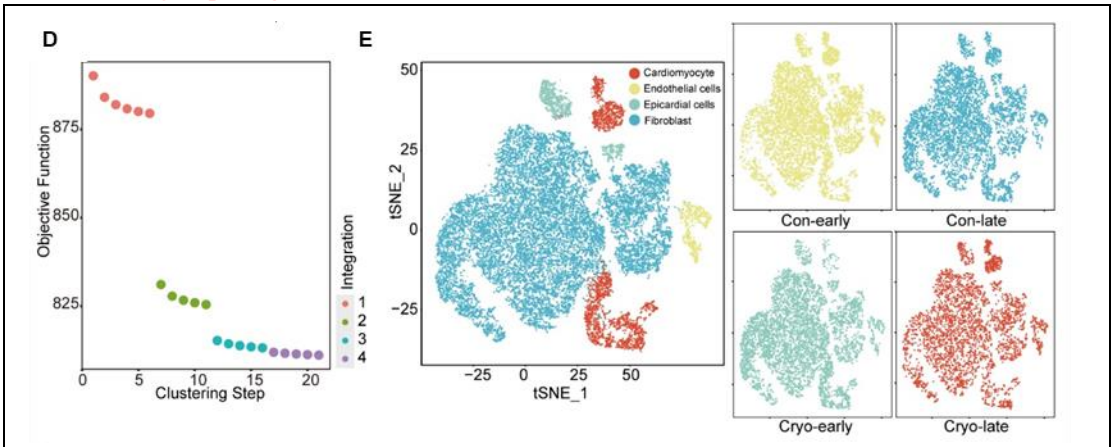

Figure S5. Clustering analysis in the scRNA sequencing dataset of the hEHT injury repair model. (D) Plot showing the convergence of the Harmony integration process, with stim as the variable to harmonize. Each point represents the cost measured after one round of clustering, with different colors indicating different harmony iterations. The x-axis represents the number of iterations, and the y-axis represents the objective cost. (E) Feature UMAP plots showing the 4 main cell clusters in control and remodeled hEHT at early and late periods. The clustering UMAP plots of different groups were shown on the right side after de-batching by Harmony.

Q2-4: 4. How does your drug specifically affect these specific clusters?

R2-4: We attempted various isolation and purification techniques to enrich the specific cell subpopulations from the cryoinjured hEHT. However, due to the limitations of the technique, we

encountered limitations in purifying and culturing the CM or FB subpopulation. By delving into the references, we have summarized the potential impact of our molecule on CM or FB and incorporated this perspective into the discussion **on Lines 606 to 618 on Page 34 in the revised manuscript:**

"The ROCK inhibitor Y27632 was reported to improve cardiac function[88] and also reduce apoptosis of transplanted CM[89] in MI mice. In the hEHT injury repair model, the ROCK/RhoA signaling-related TF BHLHE40 was upregulated in CM (**fig. S8B**) and correlated with the inflammatory response after MI[90]. The WNT/β-catenin activator CHIR99021 can promote hPSC-CM proliferation[91]. The proliferative property was represented by the upregulation of ETS1, the WNT signaling-related TF, in immature CM1 at the late stage of remodeling (**fig. S8B**), while ETS1 can directly promote cardiac development through WNT signaling[92]. Meanwhile, SB431542 inhibits the TGF-β receptor and reduces CF activation-related gene expression[93]. This is the opposite of the significant upregulation of TGFβ signaling by myoCF in cryoinjured hEHT (**Fig.3K**). In addition, myoCF also directly interacted with CM through TGFβ1(**fig. S12C**), which may induce CM stress[66]. These evidences further support the potential anti-apoptotic, pro-cardiomyocyte proliferation, and anti-fibroblast activation effects of Y27632/CHIR99021/SB431542."

The following articles were newly listed as **references**

"88. Dong LY, Qiu XX, Zhuang Y, Xue S. Y-27632, a Rho-kinase inhibitor, attenuates myocardial ischemia-reperfusion injury in rats. *Int J Mol Med* **43**, 1911-1919 (2019).

89. Zhao M, *et al.* Y-27632 preconditioning enhances transplantation of human-induced pluripotent stem cell-derived cardiomyocytes in myocardial infarction mice. *Cardiovasc Res* **115**, 343-356 (2019).

90. Xu Y, *et al.* A transient wave of Bhlhe41(+) resident macrophages enables remodeling of the developing infarcted myocardium. *Cell Rep* **42**, 113174 (2023).

91. Mills RJ, *et al.* Functional screening in human cardiac organoids reveals a metabolic mechanism for cardiomyocyte cell cycle arrest. *Proc Natl Acad Sci U S A* **114**, E8372-E8381 (2017).

92. Ruan H, *et al.* Single-cell reconstruction of differentiation trajectory reveals a critical role of ETS1 in human cardiac lineage commitment. *BMC Biol* **17**, 89 (2019).

93. Hall C, *et al.* Chronic activation of human cardiac fibroblasts in vitro attenuates the reversibility of the myofibroblast phenotype. *Sci Rep* **13**, 12137 (2023)."

Q2-5: 5. How do the transcriptome of each population of cells in your EHT change with these drug treatments

R2-5: This is an interesting and thought-provoking question. To better explain the specific roles of these small molecules in CM and CF during the remodeling process of cryoinjured hEHT, we added Y27632, CHIR99021, and SB431542 to the cryoinjured hEHT at different stages: the stress period (day 0 - day 2 after cryoinjury) and the healing period (day 2 – day 4, day 4 - day 6 after cryoinjury). Subsequently, we dissociated the hEHT at the corresponding treatment endpoints to isolate CM and FB using their differential apposition properties for bulkRNA sequencing. The relevant results were added **on Lines 471 to 512 on Pages 28 to 30 in the revised manuscript:**

"Given the significant effect of the combination treatment in promoting functional repair of injured hEHT, we performed bulkRNA-seq on CM and CF in cryoinjured hEHT sequentially treated with Y27632, CHIR99021, and SB431542 and in control hEHT correspondingly treated with

DMSO (**fig. S16A**). PCA clustering analysis showed that these interventions had reproducible and individual effects on CM and CF (**fig. S16, B and C**), with downregulation of *LIMK2* and upregulation of *LEF1*, the downstream effector of ROCK and WNT signaling, and direct downregulation of TGFβ1 indicating the efficacy of the intervention at the corresponding target signaling (**fig. S16D**). Compared to Y27632 and SB431542, CHIR99021 treatment in the late period of the injury repair process (day 2-4 after cryoinjury) exerted a stronger effect on both CM and CF (**fig. S16E**). These interventions also induced common effects, such as leading to the upregulation of *STC1* in CM (**fig. S16F**), making it more antioxidant. Meanwhile, the sustained upregulation of *TDO2*[68] (**fig. S16F**) after the CHIR99021 treatment was shown to be cardioprotective.

Furthermore, Y27632 treatment specifically downregulated *CHAC2*[69] expression in CM to reduce ROS, while the specific upregulation of *GPER1*[70] can protect CM from various stressors (**fig. S17A**). Y27632 activated both the pyruvate metabolism (*LDHA*, *SLC2A1*, *HK2*), enhanced the protection against hypoxic stress (*NDNF*, *STC1*), and prostaglandin synthesis (*PTGDS*, *PTGES*) in CM and CF (**fig. S17A**), demonstrating its potential role in promoting metabolic reprogramming of the cells in response to stress. In addition, the specific upregulation of *ACKR3*[71] and *UCP2*[72] in CF is cardioprotective (**fig. S17A**).

CHIR99021 treatment decreased the expression of the ferroptosis-related gene *ALOX15*[73] in CM while increasing the expression of the cardioprotection-related gene *SSTR2*[74], and also activation of *C5AR1*[75], which can promote cardiomyocyte proliferation after cardiac injury (**fig. S17B**). The consistent changes in ERK1/2 signaling-related genes (*NPY*, *KDR*, *CD44*, *FGF19*) in CM and CF, especially CD44 as a marker distinguishing between epicardial-like CF5 and transitional CF4, which was regionally highly expressed within the cryoinjured hEHT contributing to fibrotic scar formation (**Fig. 3, G and H**) and was downregulated in the CHIR99021 group (**fig. S17B**). Meanwhile, a series of pro-inflammatory and pro-fibrotic mediators such as *IL1B*, *IL34*, *IL17RE*, *SPP1*, and *MMP9* were downregulated in the CHIR99021 group (**fig. S17B**). The most studied MMP9[76] will promote adverse cardiac remodeling post-MI, while it was upregulated in both early and late periods of the hEHT injury repair process (**fig. S4D**). Interestingly, CHIR99021 also specifically upregulated NPNT[77] in CF, a gene associated with pro-cardiomyocyte division, and TBX5[78], a gene associated with promoting CF reprogramming to CM (**fig. S17B**).

SB431542 treatment significantly downregulated a series of genes related to ECM synthesis in CM, such as *TGFB1*, *COL1A1*, *COL5A1*, *ADAMTS8*, and *SMOC2* (**fig. S17C**), while the upregulation of EPO[79] was shown to play a critical protective role post-human MI. In addition to directly downregulating the myoCF marker *ACTA2*, SB431542 specifically downregulated the profibrotic-related genes *SMYD3*, and *RASGRF1* (**fig. S17C**). Taken together, the above results demonstrated that the prominent functional repair of cryoinjured hEHT after combination treatment was jointly achieved by the enhancement of cellular stress resistance by Y27632, the reduction of CM apoptosis and promotion of CM proliferation by CHIR99021, and the direct antifibrotic effect of SB431542."

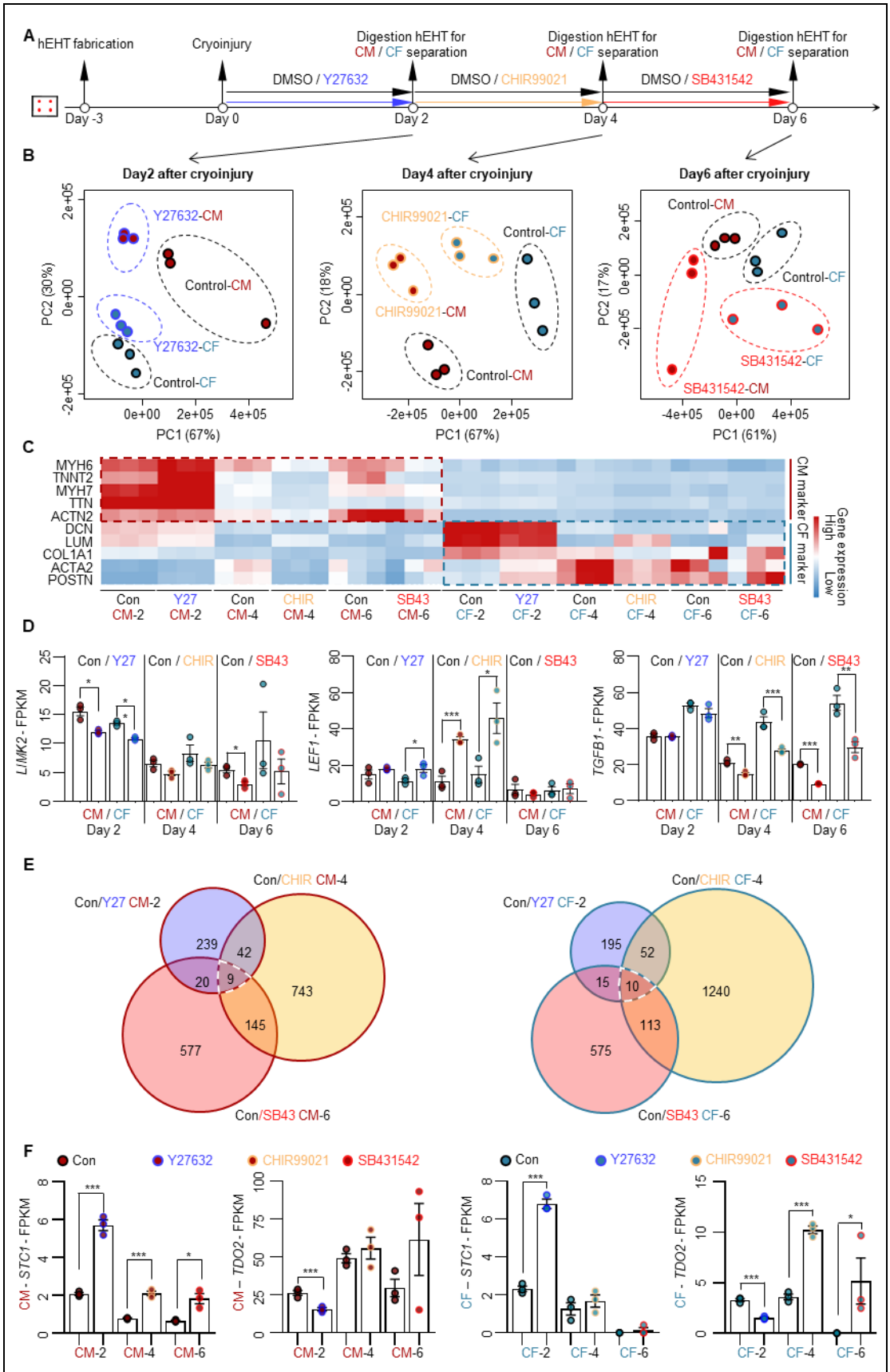

Figure S16. bulkRNA-seq analysis of CM and CF in cryoinjured hEHT treated progressively with Y27632, CHIR99021, and SB431542. (A) Flowchart of hEHT fabrication,

cryoinjury, Y27632/CHIR99021/SB435142 treatment, and CM/CF collection for bulk RNA-seq. (B) PCA scatter plot of the gene expression pattern of CM and CF samples in control (DMSO treatment on Day 2, Day 4, and Day 6 after cryoinjury) and Y27632 (Day 2, left), CHIR99021 (Day 4, middle), SB431542 (Day 6, right) group. (C) Marker gene expression heatmap for CM (*MYH6*, *TNNT2*, *MYH7*, *TTN*, *ACTN2*) and CF (*DCN*, *LUM*, *COL1A1*, *ACTA2*, *POSTN*) in different groups. (D) Differential expression of genes associated with signaling pathways targeted by small molecules between the Y27632/CHIR99021/SB431542 group and corresponding control group. (E) Venn maps of the differentially expressed genes (DEGs) in CM (left) or CF (right) between the Y27632/CHIR99021/SB431542 group and the corresponding control group. (F) The expression differences of DEGs shared by 3 pairs of control/treatment groups (*STC1* in CM, *TDO2* in CF) at day 2 (CM/CF-2), day 4 (CM/CF-4), day 6 (CM/CF-6) after cryoinjury. * $P < 0.05$; ** $P < 0.01$; *** $P < 0.001$.

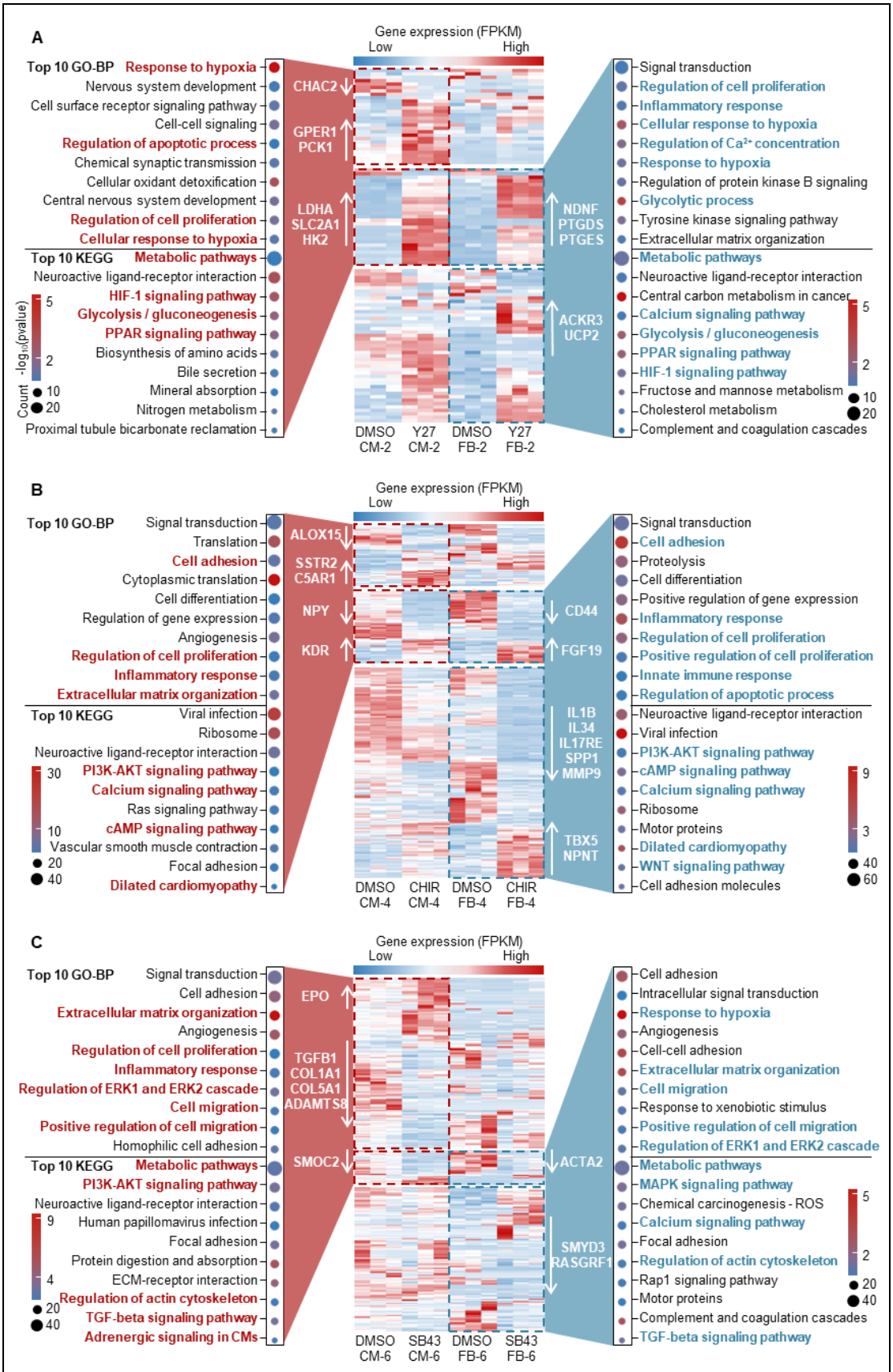

Figure S17. Transcriptomic analysis revealed the effeteness of Y27632, CHIR99021, and SB431542 in both CM and CF of cryoinjured hEHT. (A) The top 10 enriched GO and KEGG

pathways items identified from DEGs between DMSO (control) and Y27632 treated groups showed the gene expression pattern in CM (top and middle part of the heatmap) and CF (middle and bottom part of the heatmap) of hEHT at day 2 after cryoinjury. The DEGs in the middle of the heatmap were shared between the CM and CF groups. (B) The top 10 enriched GO and KEGG pathway items identified from DEGs between DMSO and CHIR99021 treated groups showed the gene expression pattern in the CM and CF of hEHT at day 4 after cryoinjury. (C) The top 10 enriched GO and KEGG pathways item identified from DEGs between DMSO and SB431542 treated groups showed the gene expression pattern in the CM and CF of hEHT at day 6 after cryoinjury. Some DEGs were listed and their expression tendencies were presented with arrows (the up arrow indicated that these genes were upregulated in the drug-treated group than the control, down arrow indicated downregulation).

The following articles were newly listed as **references**

"68. Peck KA, *et al.* Extracellular Vesicles Secreted by TDO2-Augmented Fibroblasts Regulate Pro-inflammatory Response in Macrophages. *Front Cell Dev Biol* **9**, 733354 (2021).

69. Kaur A, *et al.* ChaC2, an Enzyme for Slow Turnover of Cytosolic Glutathione. *J Biol Chem* **292**, 638-651 (2017).

70. Pei H, Wang W, Zhao D, Su H, Su G, Zhao Z. G Protein-Coupled Estrogen Receptor 1 Inhibits Angiotensin II-Induced Cardiomyocyte Hypertrophy via the Regulation of PI3K-Akt-mTOR Signalling and Autophagy. *Int J Biol Sci* **15**, 81-92 (2019).

71. Duval V, Alayrac P, Silvestre JS, Levoye A. Emerging Roles of the Atypical Chemokine Receptor 3 (ACKR3) in Cardiovascular Diseases. *Front Endocrinol (Lausanne)* **13**, 906586 (2022).

72. Cadenas S. Mitochondrial uncoupling, ROS generation and cardioprotection. *Biochim Biophys Acta Bioenerg* **1859**, 940-950 (2018).

73. Cai W, *et al.* Alox15/15-HpETE Aggravates Myocardial Ischemia-Reperfusion Injury by Promoting Cardiomyocyte Ferroptosis. *Circulation* **147**, 1444-1460 (2023).

74. Voros I, *et al.* Somatostatin and Its Receptors in Myocardial Ischemia/Reperfusion Injury and Cardioprotection. *Front Pharmacol* **12**, 663655 (2021).

75. Natarajan N, *et al.* Complement Receptor C5aR1 Plays an Evolutionarily Conserved Role in Successful Cardiac Regeneration. *Circulation* **137**, 2152-2165 (2018).

76. Lindsey ML. Assigning matrix metalloproteinase roles in ischaemic cardiac remodelling. *Nat Rev Cardiol* **15**, 471-479 (2018).

77. Meng F, Martin JF. Embryonic ECM Protein SLIT2 and NPNT Promote Postnatal Cardiomyocyte Cytokinesis. *Circ Res* **127**, 908-910 (2020).

78. Zhou Y, *et al.* Single-Cell Transcriptomic Analyses of Cell Fate Transitions during Human Cardiac Reprogramming. *Cell Stem Cell* **25**, 149-164 e149 (2019).

79. Asaumi Y, *et al.* Protective role of endogenous erythropoietin system in nonhematopoietic cells against pressure overload-induced left ventricular dysfunction in mice. *Circulation* **115**, 2022-2032 (2007)."

Q2-6: 6. Do the transcriptomic changes in the EHT reflect those seen in the MI model in vivo? I.e. how well does the EHT captures the biology as claimed?

R2-6: We compared the gene expression changes observed in both the hEHT injury repair model and the clinical MI heart to see how the in vitro model reflects reality. We referenced Rao's study[34], which reported the first single-cell transcriptome map in human ischemic cardiomyopathy. We found that the hEHT model effectively mimics the dynamics of key gene expression and signaling pathways dynamic seen in the clinical MI heart, particularly those related to CF activation and differentiation. The relevant results were added **on Lines 338 to 348 on Page 17 in the revised manuscript:**

"To assess the in vivo relevance of CF fate transition in the hEHT injury repair model, we further referenced the scRNA-seq data from clinical heart with dilated cardiomyopathy (DCM) and ischemic cardiomyopathy (ICM) hearts[34] (**fig. S11D**). Clustering and pseudotime analysis revealed that the quiescent CF in human MI hearts similarly underwent two distinct fates to transition to myoCF or contractile CF (**fig. S11, E and F**), which were regulated by TGFβ, WNT, PI3K, and ERK signaling pathways (**fig. S11G**). The CF in hEHT injury repair model showed similar fate transition patterns, including the dynamic expression of genes associated with TGF-β signaling (*JUN*, *FOS*, *COL3A1*), extracellular matrix (*ADAMTS1*, *COL16A1*, *MMP28*), and stress response (*COL1A1*, *BTG*, *FOSB*) as in vivo (**Fig. 4, C and D**). These results suggested that the hEHT injury repair model effectively captures the biological processes of CF fate transition identified in human MI."

The following article was newly listed as **references**

"34. Rao M, *et al.* Resolving the intertwining of inflammation and fibrosis in human heart failure at single-cell level. *Basic Res Cardiol* **116**, 55 (2021)."

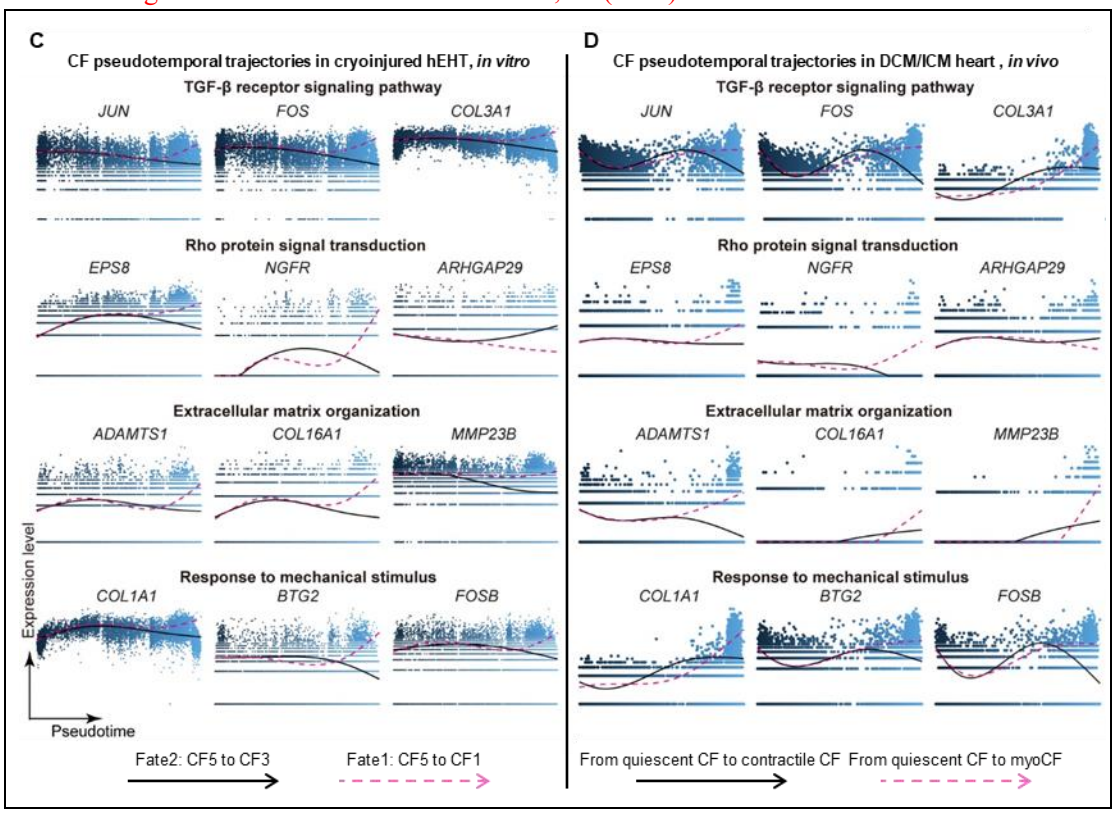

Figure 4. Pseudotime analysis revealed that CF in the hEHT injury repair model exhibited comparable cell fate transitions in vivo. (C) Spline plots of representative genes changed in two CF transition trajectories in the hEHT injury repair model. (D) Spline plots of the same genes in (C) that were changed in two CF transition trajectories in the clinically DCM/ICM hearts (GEO: GSE145154). The black line indicated the gene expression change from quiescent CF to contractile CF, and the pink dashed line indicated the change from quiescent CF to myoCF.

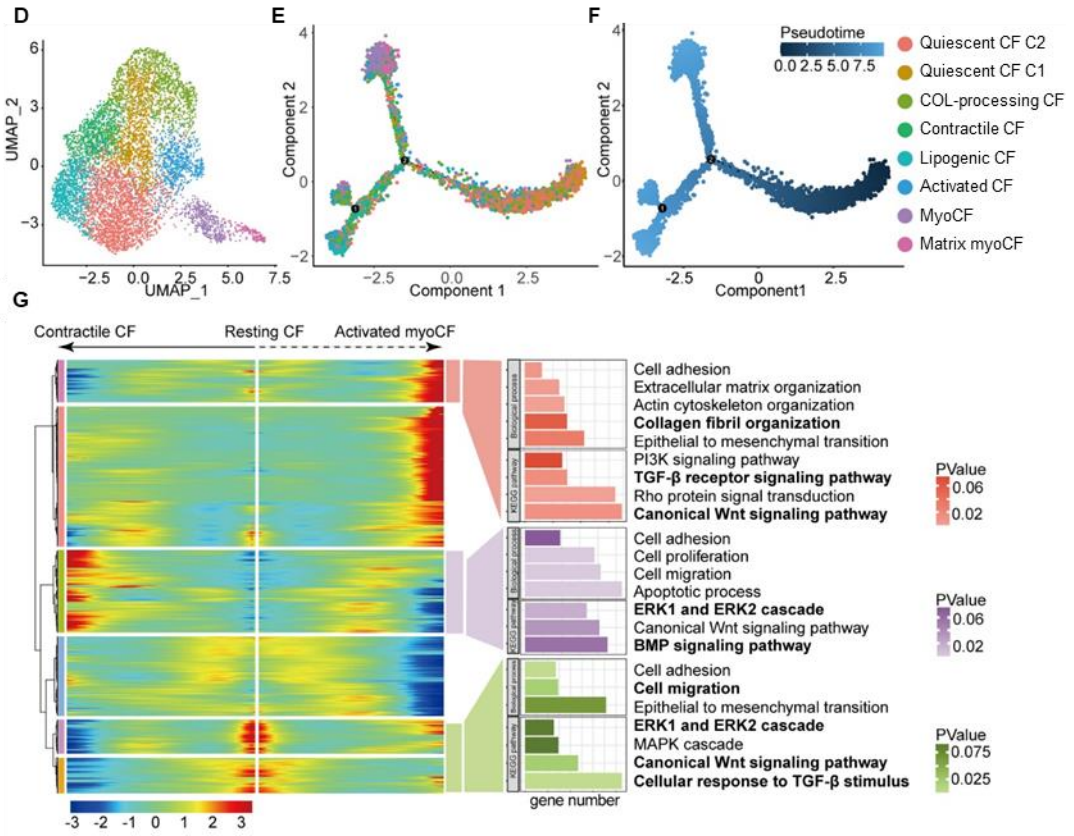

Figure S11. Pseudotime analysis of CF subpopulations in the hEHT injury repair model and clinical DCM/ICM hearts. (D) UMAP plot showing the CF clusters from the scRNA sequencing database of normal, DCM, and ICM hearts (GEO: GSE145154). (E) Distinct states of CF subpopulations identified by pseudotime analysis in clinically normal, DCM, and ICM hearts. (F) Pseudotemporal trajectory plot of CF in clinically normal, DCM, and ICM hearts. (G) Heatmap of significantly changed genes at the transition node (position 2 in (F)) from quiescent CF to activated myoCF or contractile CF. The color from blue to red indicated the relative expression level from low to high. Representative GO terms of the significantly changed gene set in pseudotime trajectory were shown on the right.

Q2-7: 7. Has the authors tried other 3-factor combinations from the original screen? Or are the three factors chosen because they each had some perceived partial benefits, so combination must be better? This three-compound approach is highly unlikely to be translatable.

R2-7: Thank you for your detailed and considerable comments. We screened 17 compounds that activate or inhibit various signaling pathways to identify potential treatments to enhance myocardial recovery (**Fig. 6A, original Fig. 5A**). We evaluated the effect of these compounds on preventing CF overactivation and promoting myocardial repair in situ using three assessment indices: the length of activated CF stress fibers, the percentage of CM, and the degree of CM eccentricity in the remodeled area (**fig. S14, B and C, original fig. S9, B and C**).

Of the 17 compounds, Y27632, CHIR99021, SCH772984, and SB431542 were found to reduce the length of CF stress fibers in the remodeled area and promote the orientation of CM toward the remodeled area, and increase the percentage of CM in the area (**Fig. 6D, original Fig. 5D**). However, SCH772984 was found to promote CM contraction, which could potentially increase the area of injury and lead to rupture. As a result, Y27632, CHIR99021, and SB431542 were logically selected for further evaluation and experimental validation in vivo.

Since the myocardial remodeling process occurs in different periods and continuous dosing may lead to unexpected side effects, we designed a combination treatment strategy focusing on early anti-apoptosis, mid-term promotion of myocardial regeneration, and late inhibition of excessive fibrosis.

Q2-8: 8. All three compounds seems to significantly reduce infarct size! That's quite impressive (figure 7F). What's the P value for those other ones? Has this been confirmed?

R2-8: Only the combination treatment can significantly reduce the infarct size compared to the vehicle (**fig. S19F, original Fig. 7F**), its P value was 0.0125. The P=0.0518 in the Y27632 group, P=0.2040 in the CHIR99021 group, and P=0.3878 in the SB431542 group, these sustained single-factor treatment groups only tended to reduce infarct size compared to the vehicle group. Another reviewer suggested that giving the wrong treatment at the wrong time could cause potential side effects, which prompted us to design additional experiments in adult MI mice. This experiment further confirmed the superior effect of the combination treatment in promoting cardiac functional repair of MI mice compared to staged single-factor treatments. The relevant results were added **on Lines 531 to 547 on Pages 30 to 31 in the revised manuscript:**

"Subsequently, we developed the MI model in adult mice and evaluated the therapeutic effects of Y27632, CHIR99021, SB431542, and their combination (**Fig. 8A**). Echocardiography assessment (**Fig. 8B**) revealed that both the ejection fraction (EF) and fractional shortening (FS) significantly decreased in all treated groups compared with the sham-operated group at day 1 post-MI. However, only the combined treatment enhanced cardiac function considerably after 21 days post-treatment compared to the vehicle group (**Fig. 8, C, and D**). The Masson staining analysis (**Fig. 8E**) further showed the combined treatment can significantly reduce the fibrotic area compared to the vehicle group (**Fig. 8F**). Notably, the phased single-factor treatment with CHIR99021 in days 7 to 14 (cardiac replacement fibrosis phase) post-MI also significantly reduced the formation of fibrotic scar (**Fig. 8F**) but failed to rescue the cardiac function (**Fig. 8, C and D**). In contrast, sustained CHIR99021 treatment throughout the remodeling process (21 days post-MI) in adult MI

mice (**fig. S19A**) failed to reduce the fibrotic area. In contrast, phased interventions in combination with Y27632, CHIR99021, and SB431542 can still promote functional repair post-MI (**fig. S19, B to F**), indicating the importance of symptomatic treatment of remodeling stages with different pathological features. The above results further validate that the potential value of the Y27632, CHIR99021, and SB431542 identified from the hEHT injury repair model, their combination can distinctively have a positive impact on MI." fig. S19 is the original Fig. 7.

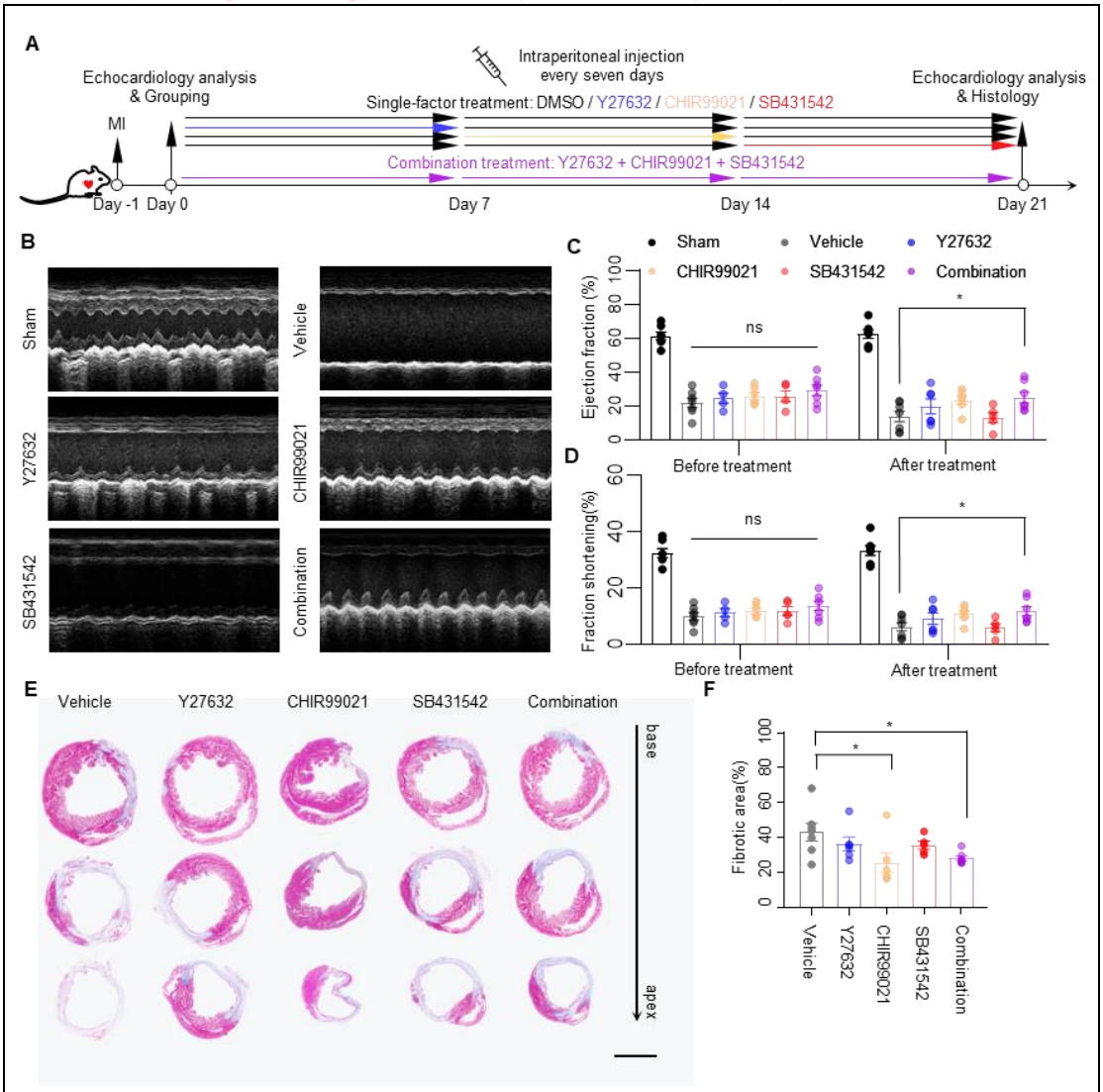

Figure 8. The combination treatment reduced the fibrotic area and improved cardiac function in the adult mouse model of MI. (D) Schematic of different treatments (DMSO, Y27632, CHIR99021, SB431542, and their combination) in adult mice after MI. (E) Representative images of M-code echocardiography from Sham, Vehicle, Y27632, CHIR99021, SB431542, and their combination-treated mice after 21 days of treatment. (F) Ejection fraction measured by echocardiography in different groups of mice before treatment and 21 days after treatment. (G) Fraction shortening measured by echocardiography in different groups of mice before treatment and 21 days after treatment. n=7 mice for Sham, Vehicle and Combination; n=6 mice for Y27632 and CHIR99021; n=5 mice for SB431542. (H) Representative Masson staining images of heart sections from different groups of adult mice at 21 days after treatment. Scale

bar,2.5mm. (I) Quantitative analysis of fibrotic area measured from Masson staining image from different group mice at 21 days after treatment. n = 7 mice for Vehicle and Combination; n=6 for Y27632 and CHIR99021; n = 5 mice for SB431542. ns, not significant; *P < 0.05. **P < 0.01.

Q2-9: 9. How are the 17 candidates chosen? it just says 17 compound in altered pathways from RNAseq. 3/17 hits are quite incredible for any pharmacological screen for phenotype even for one pathway. What does that say about the model's sensitivity and specificity? can you utilize any positive or negative controls?

R2-9: Based on the bulk RNA-seq database, KEGG analysis of differentially expressed genes for the cryoinjured group versus the control group at early and late periods during the injury repair process showed that MAPK, cAMP, and HIF-1α pathways were enriched in the early periods (**fig. S4, E and F**). In contrast, TNF and NFκB pathways stood out in the late period (**fig. S4, E and F**). Further analysis of the scRNA-seq database revealed that WNT signaling regulated oxidative metabolism in CM during remodeling (**fig. S7, A and B, original fig. S6, A and B**). TGFβ, MAPK, PI3K, and RHO signaling were extensively involved in the hypoxic stress of different CF subpopulations in the early period (**fig. S9, A and B, original fig. S7, A and B**). Additionally, PI3K signaling was involved in regulating fibroblast proliferation in the late period (**fig. S9, C and D, original fig. S7, C and D**). Both signaling activators and inhibitors were selected to evaluate the regulatory effects of these signaling pathways on myocardial remodeling. bFGF, TGFβ1, a known activator of the fibrotic response, significantly reduced the percentage of CM in the remodeling area (**fig. S14G, original fig. S9G**). This can be considered as a negative control. Moreover, NS398 and SB431542 reduced CF activation (**fig. S14I, original fig. S9I**), while CHIR99021 and Y27632 promoted CM percentage in the remolded area (**fig. S14G, original fig. S9G**). Y27632 and CHIR99021 have been reported to promote myocardial recovery post-MI and can be considered as positive controls in our model.

Also, as you mentioned, this is an interesting tissue model for studying hPSC-CM interaction with CM. But to be honest, as our existing models are unsuitable for large molecular libraries, we tend to choose those with relevant evidence and focus on joint effects when we select candidate molecules. We will continue to enhance our system to increase its throughput and make it more suitable for compound bank screening.

2-10: 10. Beyond contractility, are the electrical / calcium phenotype also restored around the scar in the MI model with drug treatment?

R2-10: We appreciate your very constructive questions! We have taken another reviewer's valuable suggestion that we should change the continuous dosing regimen for the adult MI mice in the single factor treatment group, which is maintained for 21 days, to a 7-day phased dosing regimen, which corresponds to the combination treatment to avoid side effects associated with drug administration at the wrong time. Based on the above experimental protocol, we perfused the hearts of mice treated for 21 days with RHOD2 dye and performed optical mapping analysis. The relevant results were added **on Lines 548 to 560 on Page 32 in the revised manuscript:**

"To further assess the impact of different treatments on the recovery of the electrophysiological

function of MI mice hearts, we analyzed the calcium activity characteristics of the treated ventricles under four loading conditions using optical mapping (**fig. S20A**). In the control ventricle, as we found in the hEHT injury repair model, the area of disturbed calcium signaling progressively increased with increasing electrical pacing frequency and ISO loading (**fig. S20B**). In addition, we observed a reduction in the amplitude of calcium signaling in the disturbed area, along with the prolongation of CSD80 and the occurrence of arrhythmias in response to high-frequency pacing (**fig. S20, C and D**). The combination treatments significantly reduced the abnormal functional areas' percentage (**fig. S20B**) and improved ventricular conduction velocity and conduction direction homogeneity to normal levels (**fig. S20E**). Based on the integrated scoring system developed to evaluate all characteristic parameters related to the calcium signaling activity, the combination treatment demonstrated the best effect in rescuing the electrophysiological dysfunction in the adult infarcted mice (**fig. S20F**)."

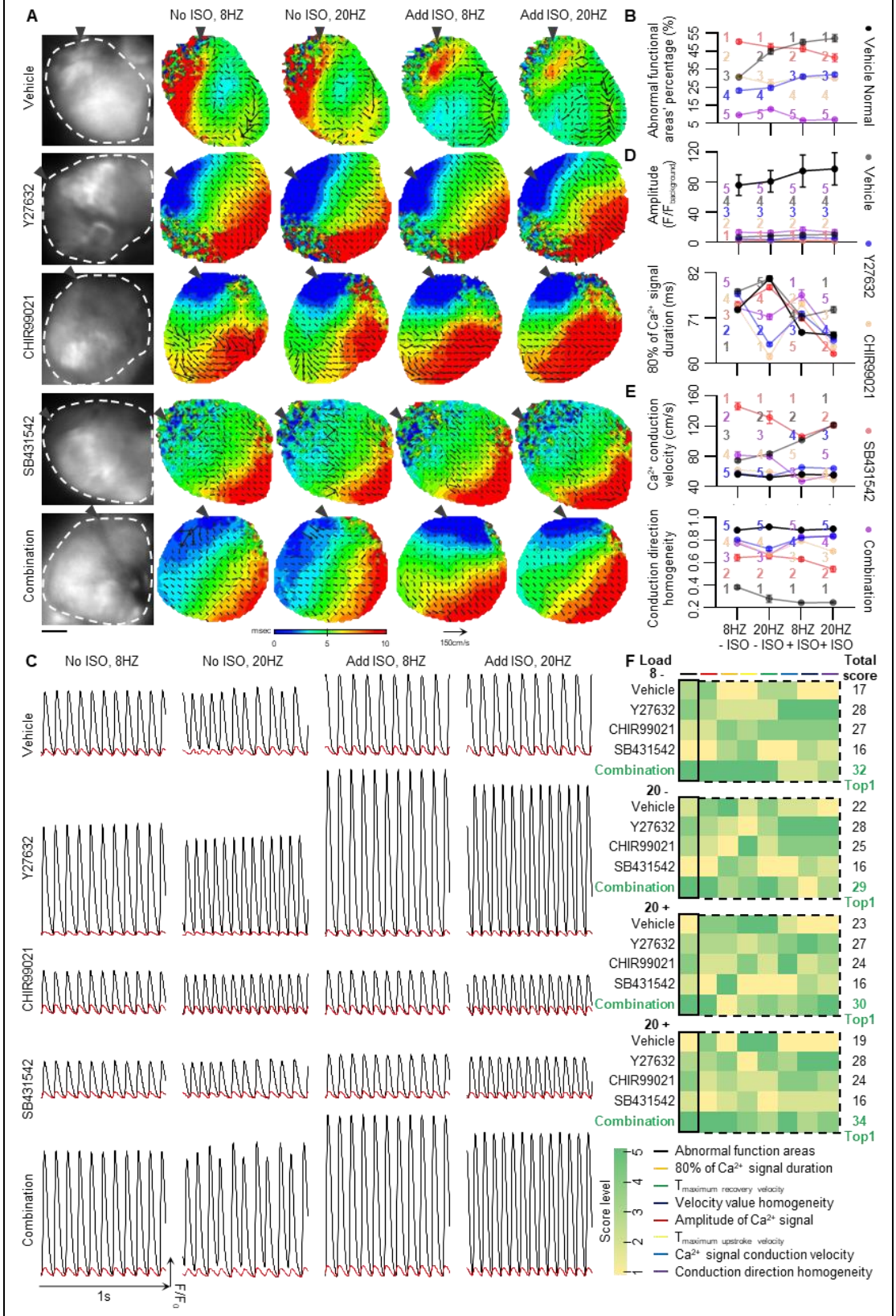

Figure S20. Figure 10. The combination treatment rescued the abnormality of calcium activity in the adult mice model of MI. (A) Representative bright field image(left) and

activation map of the infarcted mouse heart under different electrical stimulation and ISO loads (8HZ stimulation with or without ISO, 20HZ stimulation with or without ISO). The conduction velocity and direction of the calcium signal were indicated by the arrows of varying lengths. The black triangle represented the origin of electrical point stimulation (8/20HZ). Scale bar 2mm. (B) Variation in the area of the abnormal calcium activities regions under different electrical stimulation and ISO loads. n=6 infarcted areas. Different colored numbers represent the scores of different treatments under 4 loading conditions, with higher scores representing better recovery effects. (C) Representative calcium signal waveforms in the infarcted (red waveform) and remote area (black waveform) under different electrical stimulation and ISO loads. (D) Quantification of the amplitude and CSD80 of calcium signal in the infarcted areas under different electrical stimulation and ISO loads. n=6 infarcted areas. (E) Quantification of conduction velocity and direction homogeneity of calcium signal in the infarcted areas under different electrical stimulation and ISO loads. n=6 infarcted areas. (F) Integrative ranking charts are based on the difference between the 8 parameters of the infarcted area in different treatments and the remote area in the vehicle group (normal status). An increase in green intensity means the closer the corresponding parameter is to the normal, the higher the score (from 1(yellow) to 5 (green)) as the ranking number shown in the line graph of (B) to (E).

Q2-11: Minor: Line 359 "control of XYZ?" typo?

R2-11: We apologize for this error. It has been corrected **on Line 408 on Page 24 in the revised manuscript:** "…increased CM fractional volume in the remodeled area from 40% in the control to more than 60%..."

Q2-12: Line 431: Though the single-factor treatment could improve EF and FS… but your data showed NS… is this a typo?

R2-12: We are sorry for the misunderstanding caused by this sentence. We meant to say that all single-factor treatment groups had higher mean EF and FS in MI mice compared to the vehicle group, but the differences were not significant. This sentence has been removed in the revised manuscript.

Point-by-point response to Reviewer #3:

Q3-0: In this manuscript, Yang et al. demonstrated a novel human pluripotent stem cell-derived engineered heart tissue patch (hEHT-MI, cryoinjured hEHT model) to mimicking the post-MI pathological remodeling and electrophysiological malfunction, which can be potentially used for screening for anti-fibrotic and cardiac regeneration drugs. RNA sequencing analysis revealed a significant difference in gene expression patterns/signaling pathways at different remodeling periods of cryoinjured hEHT. Single-cell RNA sequencing of CMs and CFs indicates the different signaling pathways, like TGFb, PI3K/AKT, WNT, NFkB, cAMP, RHO and MAPK signaling pathways, play a significant role in fibrotic process, which may be potential therapeutic targets for post-MI cardiac remodeling. Using in vitro mini hEHT-MI model and in vivo mice MI model, they demonstrated the therapeutic benefit of combination treatment with TGFb inhibitor (SB431542), Rho-kinase inhibitor (Y27632), and WNT activator (CHIR99021), which could restore post-injury myocardial functional.

Overall, the study developed an in vitro humanized cardiac screening platform to develop potential protective drugs against ischemic heart disease. The manuscript is very well written and the experiments are appropriately conducted to justify the findings, which support their conclusion. I have few minor suggestions to improve the manuscript for publication.

R3-0: Thank you for the accurate and comprehensive description of our work! We are encouraged by your comments to describe our work as "The manuscript is very well written, and the experiments are appropriately conducted to justify the findings".

1. Please define the abbreviation "PDMS" in the line 133.

R3-1: Thanks for pointing this out! We have added the full name of PDMS **on Line 132 on Page 5 in the revised manuscript:** "…used along with a polydimethylsiloxane (PDMS) pedestal (**fig. S1B**) to assist cryoinjury device in localization and penetration of hEHTs (**fig. S1C**)."

2. In the Figure 1D, TUNEL positive cells are hard to be identified in the picture (in gray color), but in Figure 1E, % of TUNEL positive cells are above 20% in remodeling area and 10% in uninjured area. Please improve the quality of the picture for confirming the Figure 1E.

R3-2: We apologize that we chose an inappropriate color that resulted in illegible details in Fig.1E. As shown below, we chose magenta to indicate $TUNEL^+$ cells and improve the quality of the image. It would be clearer if you zoomed in.

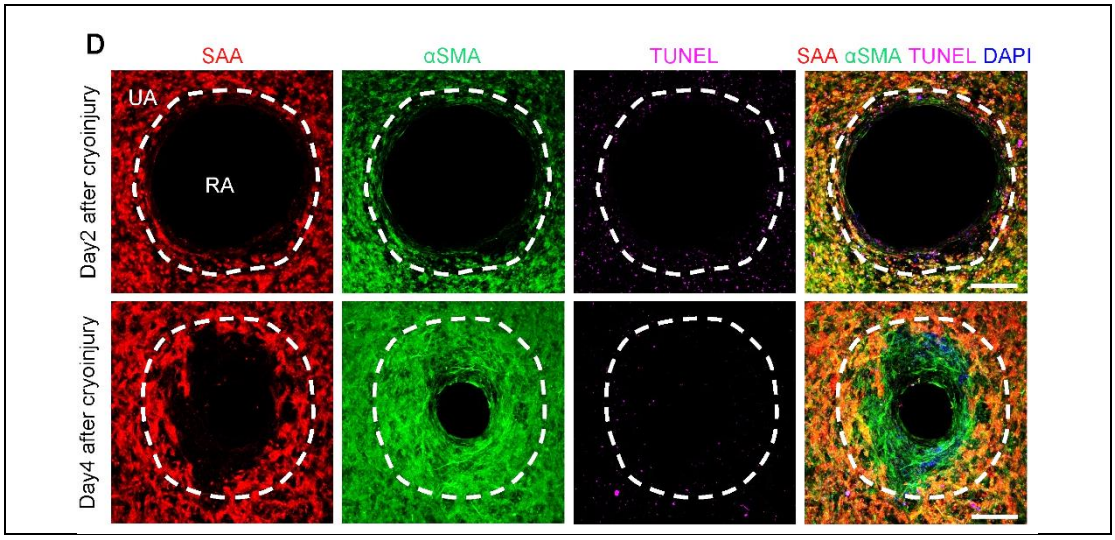

3. In line 164, collagen I is missing in "with increased deposition of collagen and III".

R3-3: Thanks very much for your review, we have corrected this omission **on Line 167 on Page 8 in the revised manuscript**: "…with increased deposition of collagen I and III in the myocardium scar."

4. Please explain why both the PI3K activator, 740YP and PI3K inhibitor, LY294002, could significantly accelerate the remodeling processes (Fig. S8C).

R3-4: The cryoinjured hEHT underwent a graded injury repair process, i.e., the cryoinjury-induced parenchymal defect expanded on day 0 to day 2 after cryoinjury and then progressively filled in over 2-4 days to form a fibrotic scar. The PI3K activator, 740YP, shortened the days required for the cryoinjured hEHT to expand to fully repair, thereby accelerating the remodeling process. Meanwhile, the PI3K inhibitor, LY294002, exacerbated the expansion of the cryoinjured area from day 0 to day 2 but still took a similar amount of time as the control group to fully refill a much larger cryoinjured area. A more systematic explanation was added **on Lines 384 to 390 on Page 22 in the revised manuscript**: "Their roles in the early and late remodeling process revealed that bFGF and LY294002 could significantly enlarge the cryoinjured area in the early period, and the remodeling process was completed before day 4 as the control group, but DMU212, 740YP, SB431542, and Y27632 directly shortened the healing time to day 3 (**fig. S13, C and D**). Thus, these interventions all exhibited the effects of accelerating the remodeling rate of injured hEHT, implying that they affect remodeling outcomes by regulating CM or CF individually in the hEHT injury repair model."

5. In figure 7E and F, % infarct size was calculated as % of total left ventricle wall area. They should provide the % of Risk area.

R3-5: We apologize for the incorrect description of the calculation of "infarct size" in our previous method. To avoid ambiguity, we have changed "infarct area (%)" to "fibrotic area (%)" in the corresponding figure (**fig. S19F, original Fig. 7F; fig. S18C; Fig. 8F.**), and used a more accurate

machine learning-based tool, the FibroSoft[96] to calculate the fibrotic area in the subsequent histological analysis. The corresponding method was corrected **on Lines 835 to 838 on Page 41 in the revised manuscript**: "Fibrotic area was calculated as the average percentage of collagen fiber area in each of the three left ventricular sections to the total area of the left ventricular wall. The percentage of the collagen fiber area was identified and calculated using the machine learning-based tool FibroSoft[96] and Image J software."

The following article was newly listed as **references**

"96. Remes A, *et al.* Adapted clustering method for generic analysis of histological fibrosis staining as an open source tool. *Sci Rep* **13**, 4389 (2023)."

REVIEWERS' COMMENTS

Reviewer #1 (Remarks to the Author):

In this revised manuscript, the authors have addressed my concerns by providing new data, offering clarifications, and including additional discussion. The new data provided in response to R1-2 enhances the rigor of the study. R1-3 has been satisfactorily addressed through new analyses of their single-cell data, particularly with the use of suggested algorithms for data integration, the addition of GRN, and pseudotime reconstruction. R1-4 has been addressed by providing key control data and establishing a more comparable neonatal cryoinjury model. However, R1-1 has only been moderately addressed. Nevertheless, I acknowledge that this challenge is universal and beyond the scope of the current manuscript. To avoid any misunderstanding, I suggest the authors further tone down the conclusions drawn from this study.

Reviewer #2 (Remarks to the Author):

I appreciate the extensive revision the authors performed to answer my initial questions. The authors have done a lot of work to address the different questions. While some of these new experiments generated more questions than answers, I think there are values to the community to publish these results to the public.

Many of the new data are based off bulk RNAseq, and presented extensively in pathway analysis form. It would have been better had these additional data be performed in single cell RNAseq to better match what it is we are seeing, and identify the actual cellular changes (Lines 471 to 512 on Pages 28 to 30) Cherry picking a few genes that matches the result seem less convincing than have scRNAseq data showed drug treatment reverses changes seen on scRNA population shifts etc. But I understand there may be cost and other concerns that limits the revision experiments.

I have only a few additional minor suggestions regarding interpretation and presentation of scRNAseq data
(1) Line 232-234, Figure S5. Using harmony without showing additional cluster is not really surprising. Harmony forces datasets together and often removes any dataset specific variance. This is not a criticism, is just not a surprising finding. Perhaps one can simply get a better look at the data simply by showing the same UMAP but coloring the dots based off the different experimental conditions (while keeping shuffle=T on seurat)) This would give us a better way to see population shift in the UMAP space as presented. (I think this should be presented in the main figure to help interpret which population(s) are shifted
(2) The secondary clustering of CM and CF was described as done using "findcluster" using Seurat, yet curiously the clusters are shown using dotted lines plotted on what looks like a gradient using pseudotime or expression of an unknown gene. The authors should specify the parameters,

including PCA(s) used, and resolution that arrived at the same cluster results as presented in the initial method.
(3) I appreciate the extensive cell-cell communication analysis that was performed. It would have perhaps been better had this analysis be performed using lower cellular cluster resolution, as having multiple CM and multiple CF cluster may have muddied the picture of what are the key interactions. And while the authors postulated multiple possible interaction and effects, it would have been stronger had the authors performed validation in vitro cross-talk experiments to validate at least some of the novel hits the authors are claiming.
(4) I would heavily caution the implied cell-fate changes as implied by pseudotime analysis in the new data presented in S11. S11(a) for example, suggest CF5 goes to CF1 and CF2. This may or may not be true and is not critical for the author's conclusions. Removing these cell-fate inference is likely prudent.
(5) Likely typo: Figure S17 tile. Transcriptomic analysis revealed the "effeteness" of Y27632. Author probably meant effectiveness

Reviewer #3 (Remarks to the Author):

All my concerns have been properly resolved. I don't have any more comment.

Black text indicates reviewer critique.

Blue text indicates responses or manuscript revisions. All new inclusions in the Revised Manuscript are highlighted in red.

Point-by-point response to Reviewer #1:

Q1-0: In this revised manuscript, the authors have addressed my concerns by providing new data, offering clarifications, and including additional discussion. The new data provided in response to R1-2 enhances the rigor of the study. R1-3 has been satisfactorily addressed through new analyses of their single-cell data, particularly with the use of suggested algorithms for data integration, the addition of GRN, and pseudotime reconstruction. R1-4 has been addressed by providing key control data and establishing a more comparable neonatal cryoinjury model. However, R1-1 has only been moderately addressed. Nevertheless, I acknowledge that this challenge is universal and beyond the scope of the current manuscript. To avoid any misunderstanding, I suggest the authors further tone down the conclusions drawn from this study.

R1-0: We appreciate your recognition of the improvements made under your valuable guidance. In response to your suggestions, we have streamlined the introduction and discussion sections of the revised manuscript. Specifically, we have removed the content related to the therapeutic targets identified from our hEHT injury repair model and their potential application for myocardial infarction treatment. This modification aims to prevent potential misunderstanding because the cardiomyocytes in our model do not fully attain the physiological state of adult cardiomyocytes. We believe that these changes enhance the clarity and focus of our work.

Point-by-point response to Reviewer #2:

Q2-0: I appreciate the extensive revision the authors performed to answer my initial questions. The authors have done a lot of work to address the different questions. While some of these new experiments generated more questions than answers, I think there are values to the community to publish these results to the public.

Many of the new data are based off bulk RNAseq, and presented extensively in pathway analysis form. It would have been better had these additional data be performed in single cell RNAseq to better match what it is we are seeing, and identify the actual cellular changes (Lines 471 to 512 on Pages 28 to 30) Cherry picking a few genes that matches the result seem less convincing than have scRNAseq data showed drug treatment reverses changes seen on scRNA population shifts etc. But I understand there may be cost and other concerns that limits the revision experiments.

R2-0: In our initial revised manuscript, we sought to demonstrate the varying interventional effects of Y27632, CHIR99021, and SB431542 on cardiomyocytes and fibroblasts through bulk RNA sequencing of isolated cardiomyocytes and fibroblasts from human engineered-heart tissue under different treatments. As you correctly identified, single-cell RNA sequencing is a more convincing approach for illustrating the recovery effects of different interventions on distinct cellular subtypes. We appreciate your final comprehension of the difficulties we have encountered, that is single-cell RNA sequencing is prohibitively expensive in terms of time and cost. In the future, we will continue to explore the detailed mechanisms of these targets in both human myocardial injury repair models and animal infarction models.

Q2-1: I have only a few additional minor suggestions regarding interpretation and presentation of scRNAseq data

(1) Line 232-234, Figure S5. Using harmony without showing additional cluster is not really surprising. Harmony forces datasets together and often removes any dataset specific variance. This is not a criticism, is just not a surprising finding. Perhaps one can simply get a better look at the data simply by showing the same UMAP but coloring the dots based off the different experimental conditions (while keeping shuffle=T on seurat)) This would give us a better way to see population shift in the UMAP space as presented. (I think this should be presented in the main figure to help interpret which population(s) are shifted.

R2-1: We sincerely appreciate your comprehensive assessment of our manuscript. Another reviewer initially proposed the suggestion to use Harmony for clustering to determine the existence of any injury-specific cell subpopulations. Following your insightful feedback, we have incorporated UMAP plots colored by experimental conditions such as Fig. 3a and b, allowing for visual inspection of potential population shifts. The relevant results have been added **on lines 204 to 205 on Page 12 in the revised manuscript:**

"Meanwhile, the UMAP plots separated across varying groups illustrating cryoinjury didn't yield new cell subpopulation (Fig. 3a, b)."

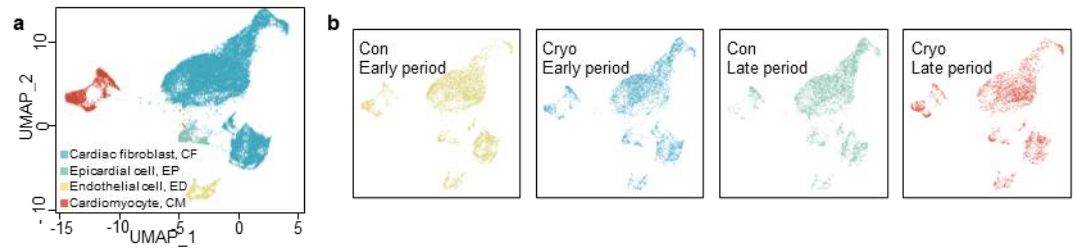

Figure 3. Transcriptomic analysis underlying the subcellular composition and signaling dynamics during the remodeling of injured hEHT. a. UMAP plot showing the four main cell clusters from scRNA-seq of control and cryoinjured hEHT at early and late periods. b. Feature UMAP plots demonstrating the four cell clusters in each group…

Q2-2: (2) The secondary clustering of CM and CF was described as done using "findcluster" using Seurat, yet curiously the clusters are shown using dotted lines plotted on what looks like a gradient using pseudotime or expression of an unknown gene. The authors should specify the parameters, including PCA(s) used, and resolution that arrived at the same cluster results as presented in the initial method.

R2-2: We apologize for the misunderstanding caused by the dotted line, which was intended to facilitate readers to identify the various cell subpopulations. The secondary clustering UMAP plots of CM and CF have been revised by removing the dotted line (Fig. 3c, e, g, i). Additionally, the parameters used for the secondary clustering have been clarified in the methods section **on lines 859 to 862 on Page 44 in the revised manuscript:**

"Second-level clustering was applied to both CM and CF, using 20 dimensions for clustering. A clustering resolution of 0.22 was used for CF, while a resolution of 0.5 was applied for CM. UMAP was utilized to visualize the result."

Q2-3: (3) I appreciate the extensive cell-cell communication analysis that was performed. It would have perhaps been better had this analysis be performed using lower cellular cluster resolution, as having multiple CM and multiple CF cluster may have muddied the picture of what are the key interactions. And while the authors postulated multiple possible interaction and effects, it would have been stronger had the authors performed validation in vitro cross-talk experiments to validate at least some of the novel hits the authors are claiming.

R2-3: We are grateful for your insight and feedback on our analysis of cell-cell communication. We recognize the importance of your suggestion concerning cluster resolution. In response, supplementary analyses were conducted at a lower cellular cluster resolution to better represent the interactions. We conducted a comparative analysis of the interactions by overlapping these interactions identified at both high and low cellular cluster resolutions. This method permitted the verification of the robustness of our findings and the confirmation that critical interactions were consistently observed across different resolutions. The relevant results have been added **on Lines 311 to 325 on Pages 17 to 18 in the revised manuscript:**

"Given CF's highly plastic and dynamic nature, cell interaction analysis at both the major (Supplementary Fig. 12a) and subtype level (Supplementary Fig. 12b) revealed a notable alteration in the number of CF-CM interactions post-cryoinjury, especially between CF2/CF5 and CM, except mature CM3 (Supplementary Fig. 12c). To focus on the most representative interactions, the injury-specific cell interactions between CF and CM were further investigated at the subpopulation level (Supplementary Fig. 12d). In the early period of remodeling, the APOA2_ABCA1 interaction was enhanced between CF2/5 and CM2/4, which is known to regulate CM metabolism[57]. The cryoinjury also strengthened interactions between CF5 and immature CM1/2 or proliferating CM4 via NRXN2_DAG1 (Supplementary Fig. 12e), which can promote CM proliferation[58]. CF2 continuously expressed TGFB1 to induce CM stress[59] in both the early and late period (Supplementary Fig. 12e). Meanwhile, the detrimental effects of CF2 on CM were evidenced by the increased expression of THBS1 in the late period (Supplementary Fig. 12e), which can trigger CM autophagy[60]. Conversely, FB5 exhibited a protective effect through increased DKK1_LRP6 interaction with CM (Supplementary Fig. 12e), leading to the inhibition of CM apoptosis[61]."

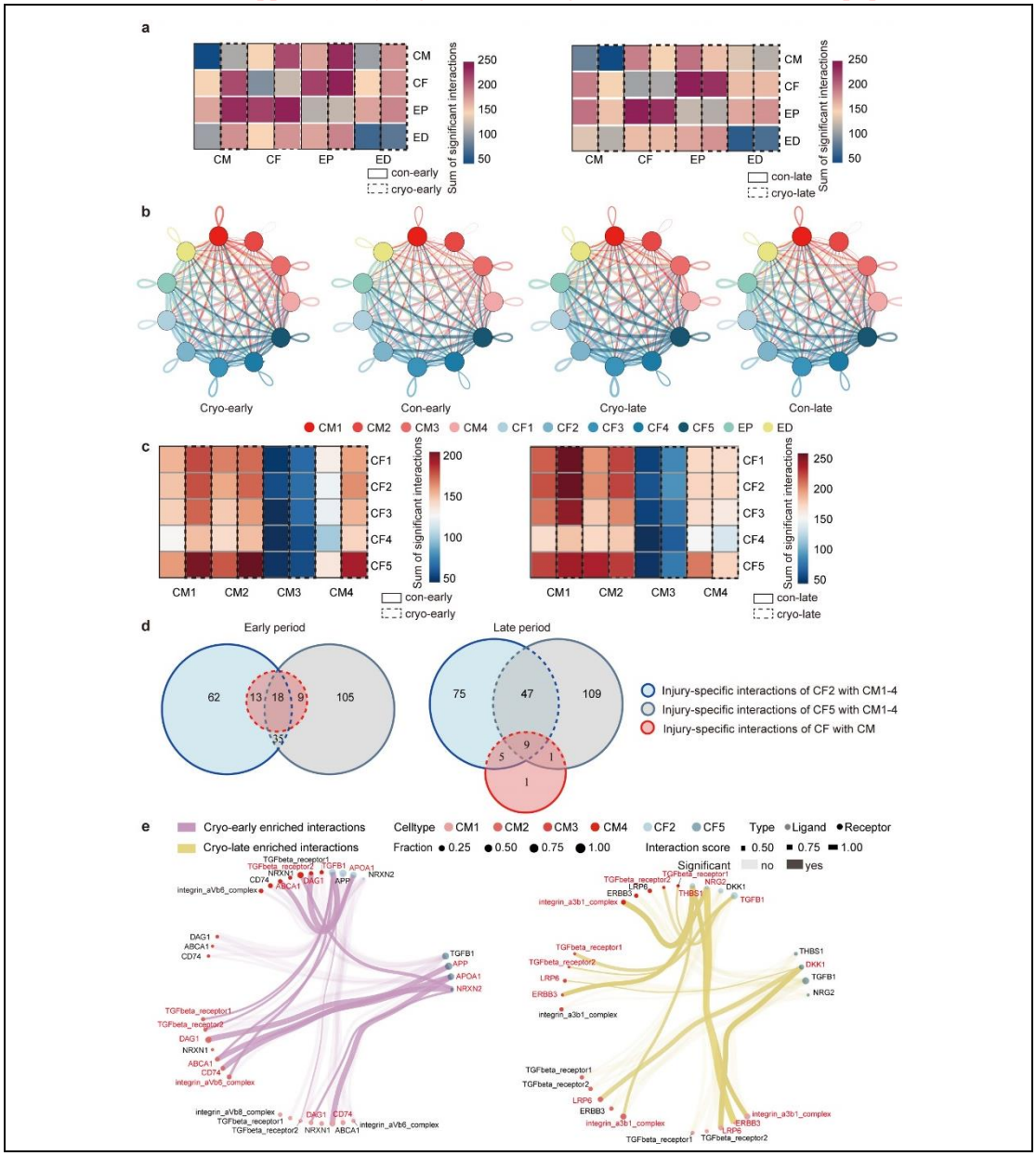

Supplementary Figure S12. Cellular interactions in the hEHT repair model. a. Heatmap of the number of CF and CM interactions in the control and cryoinjury group. **b.** The interaction network among cellular subpopulations in control and cryoinjury group at early and late periods, with connection thickness indicating interaction number. **c.** Heatmap of the number of CF1-5 and CM1-4 interactions. **d.** Venn diagrams illustrating the overlap of injury specific cell interactions among CF2, CF5, and major population CF with four CM subpopulations during both early and late periods of remodeling. **e.** Circle plots detailing specific interactions in the cryoinjured hEHT at early and late periods.

The following articles were newly listed as **references**

"57. Zhao GJ, Yin K, Fu YC, Tang CK. The interaction of ApoA-I and ABCA1 triggers signal transduction pathways to mediate efflux of cellular lipids. *Mol Med* **18**, 149-158 (2012).

58. Morikawa Y, Heallen T, Leach J, Xiao Y, Martin JF. Dystrophin-glycoprotein complex sequesters Yap to inhibit cardiomyocyte proliferation. *Nature* **547**, 227-231 (2017).

59. Sorensen DW, van Berlo JH. The Role of TGF-beta Signaling in Cardiomyocyte Proliferation. *Curr Heart Fail Rep* **17**, 225-233 (2020).

60. Zhou J, *et al.* The long noncoding RNA THBS1-AS1 promotes cardiac fibroblast activation in cardiac fibrosis by regulating TGFBR1. *JCI Insight* **8**, (2023).

61. Wang Y, *et al.* Low density lipoprotein receptor related protein 6 (LRP6) protects heart against oxidative stress by the crosstalk of HSF1 and GSK3beta. *Redox Biol* **37**, 101699 (2020)."

Q2-4: (4) I would heavily caution the implied cell-fate changes as implied by pseudotime analysis in the new data presented in S11. S11(a) for example, suggest CF5 goes to CF1 and CF2. This may or may not be true and is not critical for the author's conclusions. Removing these cell-fate inference is likely prudent.

R2-4: In the first round of review, we performed pseudotime analysis based on our scRNAseq data as suggested by another reviewer, and for the analysis results we provided, this reviewer thought that we had satisfactorily resolved his concern about cell fate transition during myocardial injury repair. Meanwhile, CD44, as a marker of transition state CF4 (Fig. 3g), was spatially specifically highly expressed in the remodeled area (Fig. 3j, k), and its opposite trend existed in the different fate transitions from epithelial-like CF5 to quiescent CF3 and active CF1, i.e., activated CF1 had higher CD44 expression compared to quiescent CF3 (Supplementary Fig. 11c), which was consistent with our observation by immunofluorescence that CD44 expression first increased (from low CD44 expression by quiescent CF3 in the uninjured area to high CD44 expression by transition CF4 at the edge of the remodeled area) and then declined (from high CD44-expressing CF4 to the relatively low CD44-expressing activated CF1-2 at the center of the remodeled area) along the remodeled area of the injured hEHT. The above results partially validated our analysis of CF fate transitions. They demonstrated that our hEHT repair model could be a potential platform to study cell fate transitions during myocardial injury repair. Nevertheless, we agree with you that "this may or may not be true," so we have simplified the description of the cell fate transition analysis in the revised manuscript.

Q2-5: (5) Likely typo: Figure S17 tile. Transcriptomic analysis revealed the "effeteness" of Y27632. Author probably meant effectiveness

R2-5: We apologize for this error and have fixed it in the revised manuscript.

Point-by-point response to Reviewer #3:

Q3-0: All my concerns have been properly resolved. I don't have any more comment.

R3-0: We appreciate your recognition of our work!